Electronic Supplementary Material (ESI) for Analyst.

Supplementary Information to Accompany:

Ion-Neutral Collisional Cross Sections of Carbohydrate Isomers as Divalent Cation Adducts and their Electron Transfer Products

Yuting Huang and Eric D. Dodds

Department of Chemistry, University of Nebraska – Lincoln

Lincoln, NE 68588-0304 USA

Collisional Cross Section Calibration Procedure.

1. Absolute ion-neural collisional cross section (CCS, Ω) values of calibration standards were reduced mass and charge state corrected to obtain normalized CCS values (Ω') for use in calibration:

$$\Omega' = \Omega \frac{\sqrt{\mu}}{z}$$

Here, μ is the ion-neutral reduced mass. For ion-neutral collision partners having masses of m_1 and m_2, respectively, the reduced mass is defined as:

$$\mu = \frac{m_1 m_2}{m_1 + m_2}$$

2. Traveling wave ion mobility spectrometry (TWIMS) arrival time distributions (ATDs) were centroided to obtain the apparent TWIMS drift times (t_d) for each calibration standard or analyte of interest.
3. Corrected drift times (t_d') were calculated by subtracting irrelevant ion transit times from the apparent drift times (td) according to:

$$t_d' = t_d - t_m - t_t - t_i$$

Here, t_m is mobility dead time, which depends on the length of the mobility cell (d_m; in Synapt G2 HDMS instruments, d_m = 25.4 cm) and the mobility cell travelling DC wave velocity (v_m):

$$t_m = \frac{d_m}{v_m} = \frac{0.254 \text{ m}}{v_m}$$

Furthermore, t_t is the time required for ion transit through the transfer region stacked ring ion guide (SRIG), which depends on the length of the transfer SRIG (d_t; in Synapt G2 HDMS instruments, d_t = 13.5 cm) and the transport cell travelling DC wave velocity (v_t):

$$t_t = \frac{d_t}{v_t} = \frac{0.135 \text{ m}}{v_t}$$

Finally, t_i is the time required for ion transit through the TOF interface region, which depends on the ion *m/z:*

$$t_i = k_i\sqrt{\frac{m}{z}} = \frac{k_{EDC}}{10^6}\sqrt{\frac{m}{z}}$$

Here, k_i is the TOF interface flight time constant, which is derived from the "enhanced duty cycle" constant (k_{EDC}) that is empirically determined for each individual instrument during installation.

4. CCS calibration curves were generated by plotting corrected drift times (t_d') as a function of normalized CCS values (Ω'). A power function of the form $t_d' = a\Omega'^b$ was fitted to the calibration data.
5. Calibration curves were then used to calculate Ω' values based on the experimentally determined t_d' values of analytes.
6. Analyte Ω' values were then converted to Ω values.
7. Further information on this calibration procedure can be found in previous reports by Huang and Dodds, and by Gelb *et al.*[1, 2]

References.

1. Y. Huang and E. D. Dodds, *Anal. Chem.*, 2013, **85**, 9728-9735.
2. A. S. Gelb, R. E. Jarratt, Y. Huang and E. D. Dodds, *Anal. Chem.*, 2014, **86**, 11396-11402.

Table S1. Polyalanine CCS standards used as calibrants in this work. These values were measured by Clemmer and co-workers[3] (z = 1, n = 15-19) and Bush and co-workers[4] (z = 2, n = 11-26) using drift tube ion mobility instruments with helium as drift gas.

Calibrant	Charge State (z)	n	Ω (Å²)	Charge State (z)	n	Ω (Å²)
Polyalanine	**1**	4	100.0	**2**	11	197.0
		5	114.0		12	208.0
		6	128.0		13	220.0
		7	141.0		14	232.0
		8	157.0		15	243.0
		9	170.0		16	255.0
		10	181.0		17	265.0
		11	194.0		18	276.0
		12	206.0		19	287.0
		13	217.0		20	297.0
		14	228.0		21	308.0
		15	235.2		22	317.0
		16	247.4		23	327.0
		17	256.2		24	337.0
		18	265.0		25	348.0
		19	276.3		26	358.0

References.

3. S. C. Henderson, J. Li, A. E. Counterman and D. E. Clemmer, *J. Phys. Chem. B*, 1999, **103**, 8780-8785.

4. M. F. Bush, I. D. G. Campuzano and C. V. Robinson, *Anal. Chem.*, 2012, **84**, 7124-7130.

Table S2. Data table for generating doubly charged polyalanine CCS calibration curve under the TWIMS conditions applied to doubly charged metal cation adducts of the FH isomers.

m/z	***z***	**Ω (Å²)**	t_d **(ADC Bins)**	***m*** **(u)**	***μ*** **(u)**	**Ω'** $(Å^2 \cdot u^{1/2} \cdot z^{-1})$	t_d **(ms)**	t_i **(ms)**	t_d' **(ms)**
400.717	2	197.0	36.7092	801.434	27.067	512.5	2.533	0.028	1.416
436.236	2	208.0	39.2257	872.471	27.142	541.8	2.707	0.029	1.588
471.754	2	220.0	41.9086	943.508	27.206	573.7	2.892	0.031	1.772
507.273	2	232.0	44.7952	1014.55	27.261	605.7	3.091	0.032	1.970
542.791	2	243.0	47.7792	1085.58	27.309	634.9	3.297	0.033	2.175
578.310	2	255.0	50.8579	1156.62	27.351	666.8	3.509	0.034	2.386
613.828	2	265.0	53.8817	1227.66	27.388	693.4	3.718	0.035	2.594
649.347	2	276.0	56.9612	1298.69	27.422	722.6	3.930	0.036	2.805
684.865	2	287.0	59.9813	1369.73	27.452	751.9	4.139	0.037	3.013
720.384	2	297.0	63.1347	1440.77	27.479	778.4	4.356	0.038	3.230
755.903	2	308.0	66.3597	1511.81	27.504	807.6	4.579	0.039	3.451
791.421	2	317.0	69.7374	1582.84	27.526	831.6	4.812	0.040	3.683
826.940	2	327.0	73.2500	1653.88	27.547	858.1	5.054	0.041	3.925
862.458	2	337.0	76.9625	1724.92	27.566	884.7	5.310	0.041	4.180
897.977	2	348.0	80.7811	1795.95	27.583	913.8	5.574	0.042	4.443
933.495	2	358.0	84.8581	1866.99	27.599	940.4	5.855	0.043	4.723

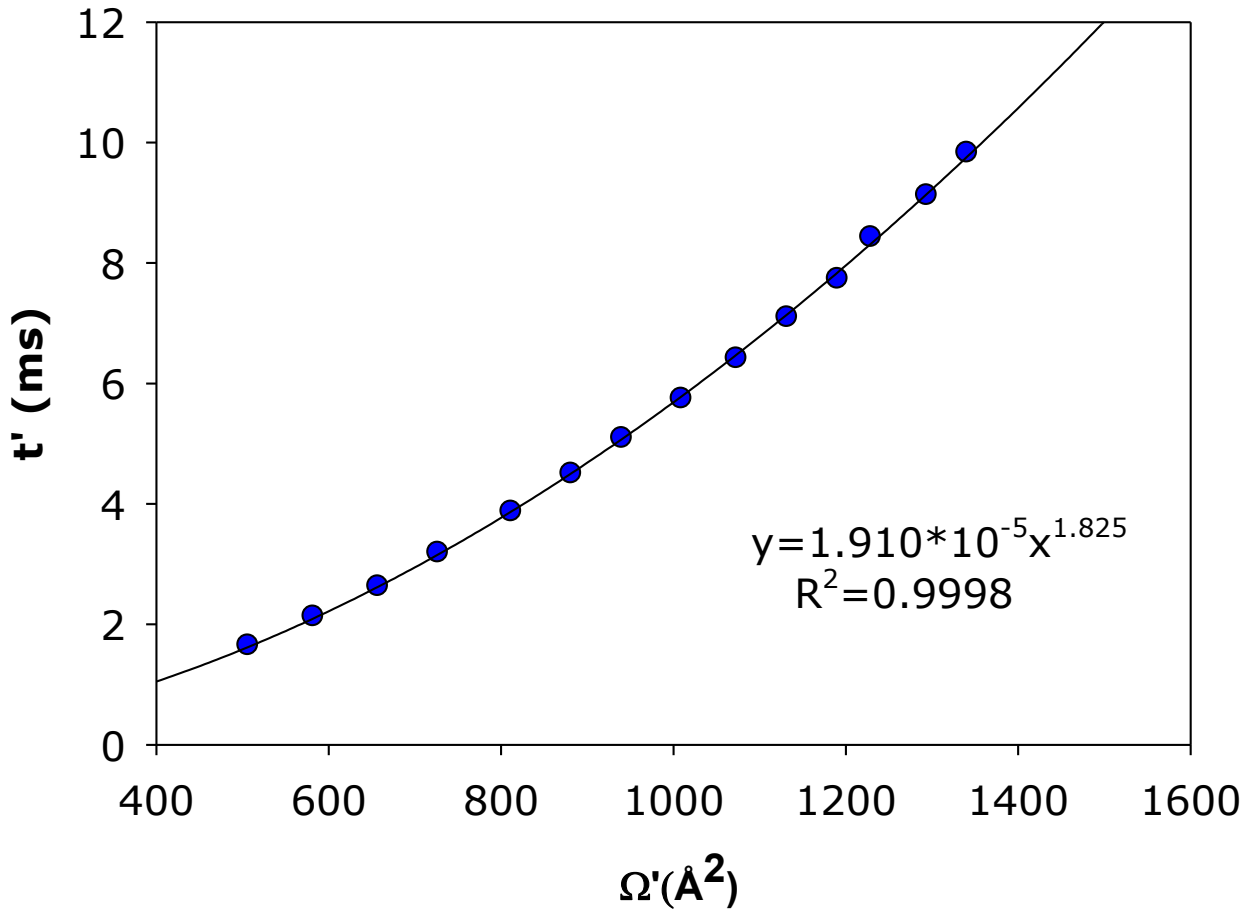

Figure S1. Representative CCS calibration curve determined under the TWIMS conditions applied to singly charged metal cation adducts of the FH isomers.

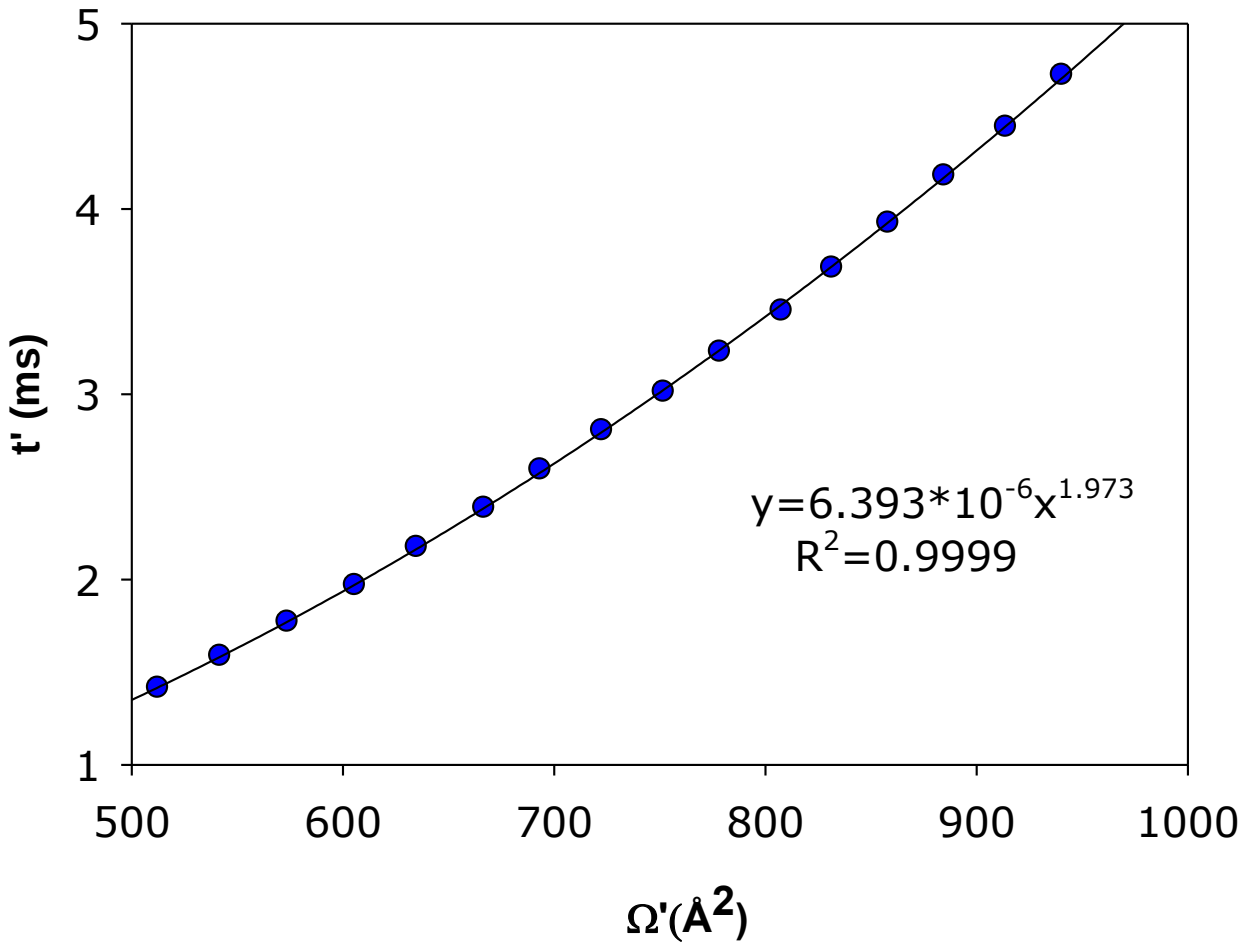

Figure S2. Representative CCS calibration curve determined under the TWIMS conditions applied to doubly charged metal cation adducts of the FH isomers.

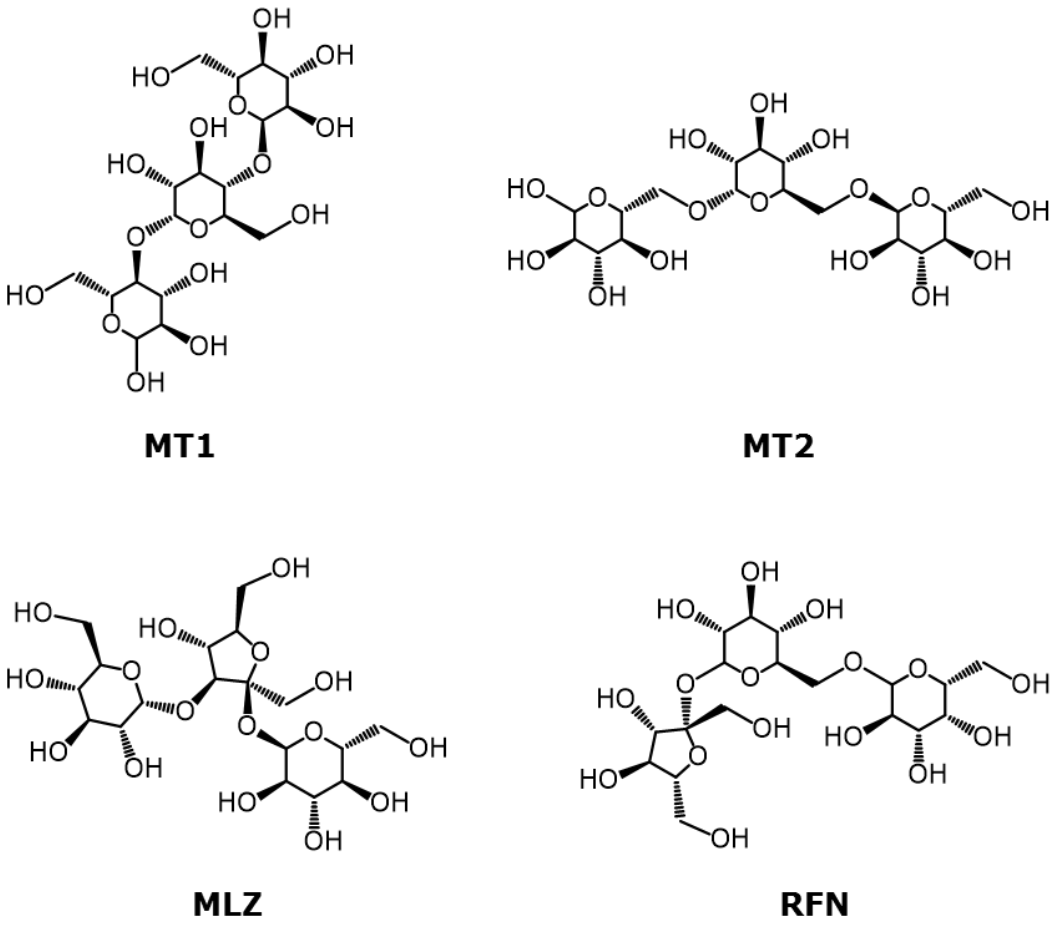

Figure S3. Molecular structures of the trisaccharide isomers maltotriose (MT1), isomaltotriose (MT2), melezitose (MLZ), and raffinose (RFN).

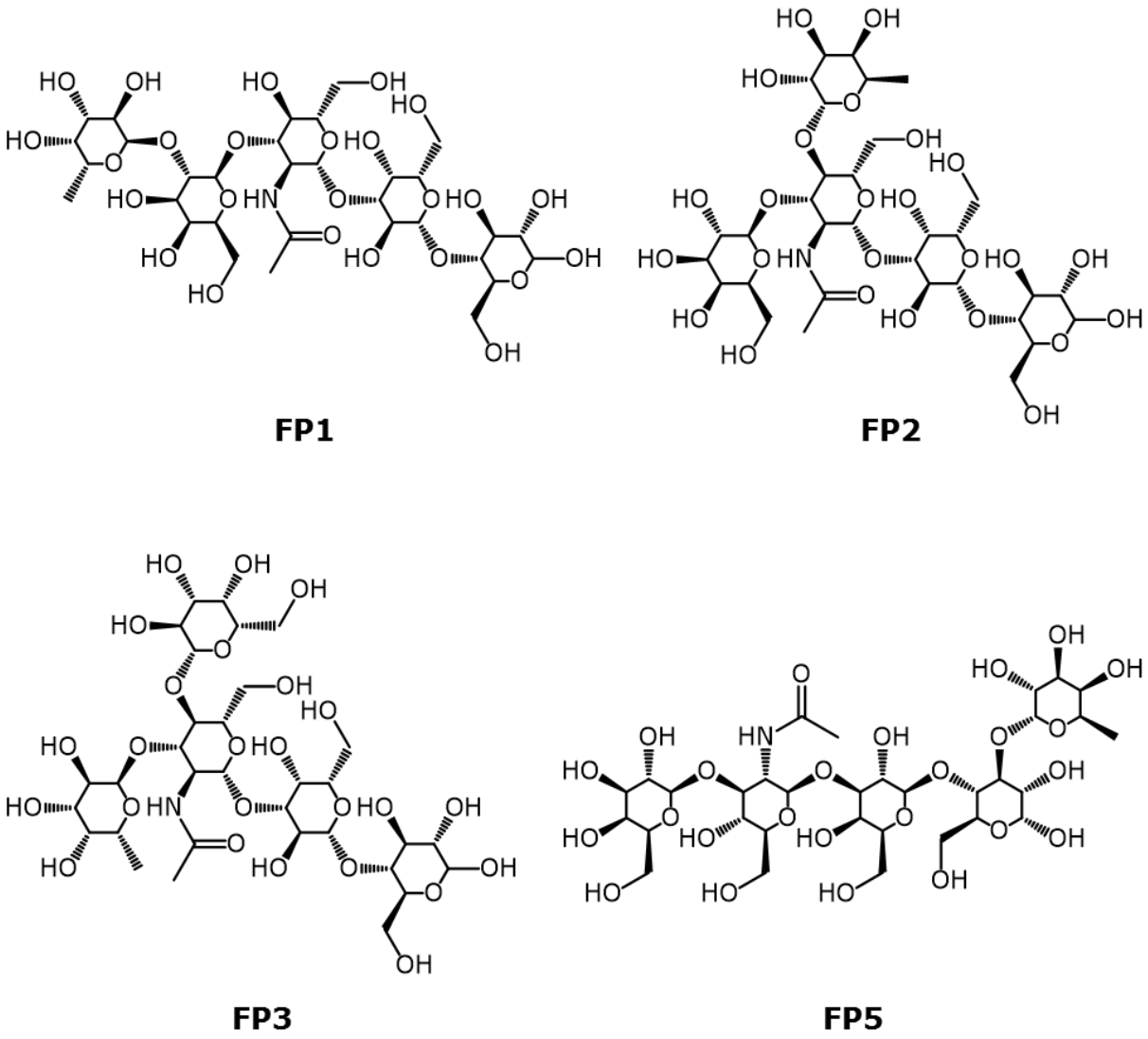

Figure S4. Molecular structures of the pentasaccharide isomers lacto-N-fucopentaose I (FP1), lacto-N-fucopentaose II (FP2), lacto-N-fucopentaose III (FP3), and lacto-N-fucopentaose V (FP5).

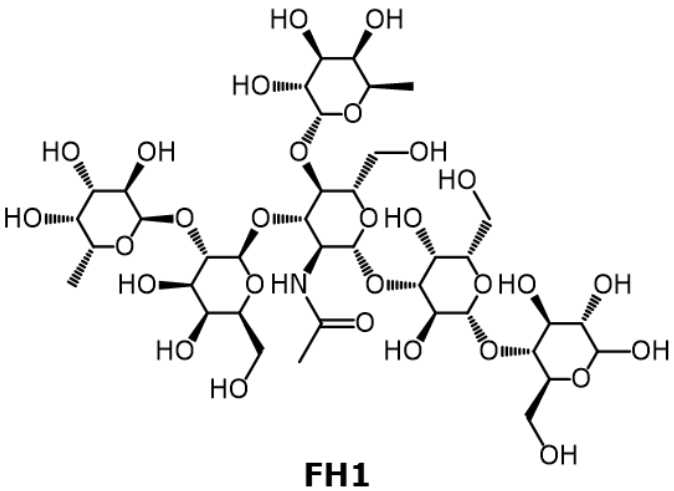

FH1

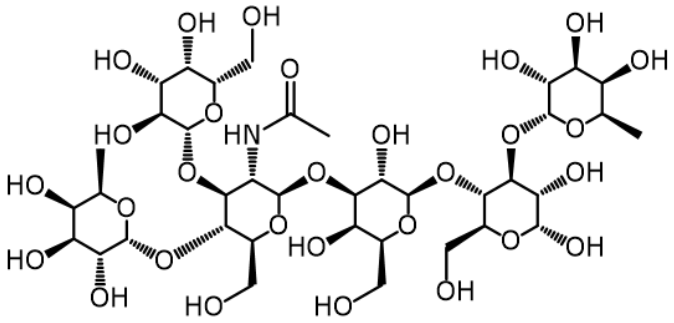

FH2

Figure S5. Molecular structures of the hexasaccharide isomers lacto-N-difucohexaose I (FH1) and lacto-N-difucohexaose II (FH2).

Table S3. Ion-neutral collisional cross sections (CCSs, Ω) of the carbohydrate / group II metal ion adducts measured in this study. The values are expressed as the mean plus or minus the standard error of the mean for four replicate measurements. For each group of isomers, the degree of polymerization (DP) is indicated.

		Ω (Å^2)				
DP	**Name**	**[M+Be]$^{2+}$**	**[M+Mg]$^{2+}$**	**[M+Ca]$^{2+}$**	**[M+Sr]$^{2+}$**	**[M+Ba]$^{2+}$**
3	**MT1**	-	136.5±0.7	136.0±0.6	139.4±0.7	142.8±1.1
	MT2	-	138.3±0.3	136.0±1.0	142.2±0.3	145.5±0.4
	MLZ	-	137.9±0.5	137.7±0.6	142.6±0.4	146.5±0.3
	RFN	-	136.2±0.3	133.6±0.4	138.4±0.6	141.3±1.1
5	**FP1**	204.0±0.3	201.1±0.4	198.2±0.8	200.8±1.0	193.5±0.9
	FP2	201.2±0.4	203.2±1.2	201.7±0.5	201.5±0.5	205.5±0.5
	FP3	201.3±0.7	199.8±0.8	195.9±0.9	196.2±1.0	197.4±1.1
	FP5	197.3±0.3	197.4±0.5	196.7±0.2	197.8±1.1	197.6±0.9
6	**FH1**	226.5±0.5	226.0±0.5	222.1±0.6	223.1±0.5	220.2±1.1
	FH2	226.5±0.4	227.2±0.8	225.5±0.5	225.7±1.4	225.5±0.9

Table S4. Ion-neutral CCSs of the electron transfer (ET) products of the carbohydrate / group II metal ion adducts measured in this study. The values are expressed as the mean plus or minus the standard error of the mean for four replicate measurements. For each group of isomers, the DP is indicated.

		Ω (Å²)				
DP	**Name**	**$[M+Be]^{+\bullet}$**	**$[M+Mg]^{+\bullet}$**	**$[M+Ca]^{+\bullet}$**	**$[M+Sr]^{+\bullet}$**	**$[M+Ba]^{+\bullet}$**
3	**MT1**	-	134.7±0.4	138.2±0.5	138.3±0.4	140.0±0.8
	MT2	-	137.1±0.2	140.2±0.2	141.0±0.3	142.9±0.1
	MLZ	-	136.2±0.3	137.7±0.4	138.7±0.2	139.4±0.3
	RFN	-	131.8±0.2	136.6±0.4	137.5±0.5	139.6±0.8
5	**FP1**	188.0±0.4	195.4±0.3	190.0±0.6	192.3±0.4	191.2±0.7
	FP2	192.6±0.5	198.2±0.2	195.6±0.6	198.3±0.6	201.0±0.5
	FP3	186.1±0.2	196.4±0.3	190.9±0.2	193.3±0.6	196.8±0.4
	FP5	198.4±0.0	198.0±0.1	198.3±0.2	196.8±0.1	194.8±0.2
6	**FH1**	212.7±0.3	217.0±0.4	213.4±0.7	215.9±0.5	216.0±0.8
	FH2	220.4±0.6	225.1±0.2	224.9±0.3	223.5±0.4	222.1±0.7

Table S5. Ion-neutral CCSs of the carbohydrate / group I metal ion adducts measured in this study and in our previous work.[1] The values are expressed as the mean plus or minus the standard error of the mean for four replicate measurements. For each group of carbohydrate isomers, the DP is indicated.

		Ω (Å²)				
DP	**Name**	**$[M+Li]^+$**	**$[M+Na]^+$**	**$[M+K]^+$**	**$[M+Rb]^+$**	**$[M+Cs]^+$**
3	**MT1**	138.6±0.2	142.9±0.2	144.4±0.2	147.0±0.3	150.8±0.2
	MT2	140.8±0.1	142.3±0.1	143.4±0.1	143.4±0.1	144.2±0.1
	MLZ	134.1±0.2	133.5±0.2	134.2±0.2	134.7±0.3	136.9±0.2
	RFN	137.3±0.4	138.8±0.4	140.0±0.4	140.5±0.4	141.8±0.4
5	**FP1**	198.1±0.2	201.5±0.3	201.1±0.3	200.8±0.2	202.0±0.6
	FP2	194.1±0.5	195.6±0.6	198.5±0.4	200.0±0.4	200.9±0.4
	FP3	192.9±0.2	196.6±0.4	194.5±0.4	195.3±0.5	195.7±0.3
	FP5	198.0±0.3	198.4±0.3	199.4±0.3	199.9±0.4	201.7±1.0
6	**FH1**	221.5±0.8	223.5±0.7	223.7±0.6	223.7±0.7	223.7±0.6
	FH2	217.7±0.3	218.7±0.3	219.9±0.3	219.8±0.2	220.4±0.2

References.

1. Y. Huang and E. D. Dodds, *Anal. Chem.*, 2013, **85**, 9728-9735.

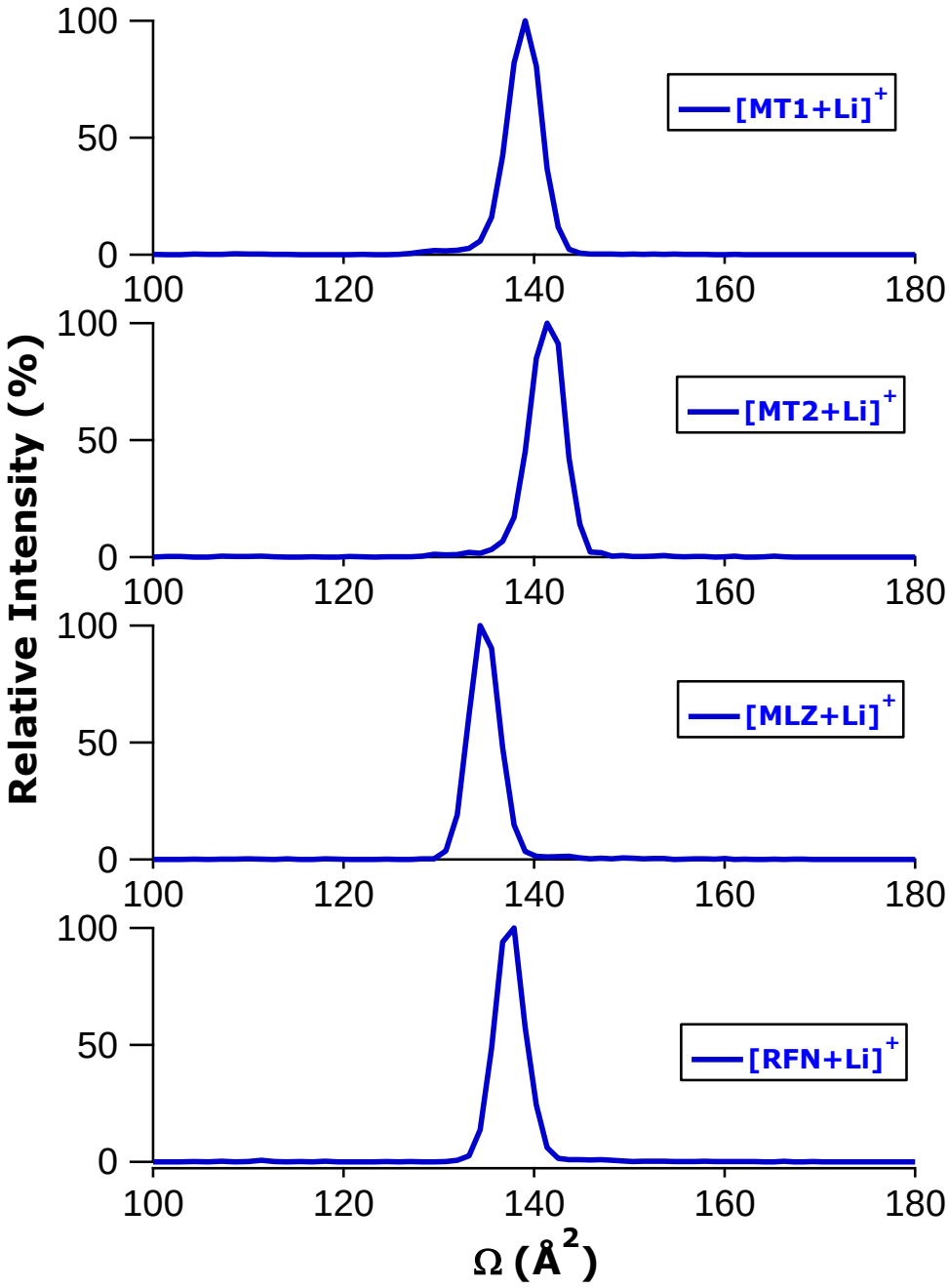

Figure S6. Representative distributions of ion-neutral CCS values for MT1, MT2, MLZ, and RFN as their lithium ion adducts.

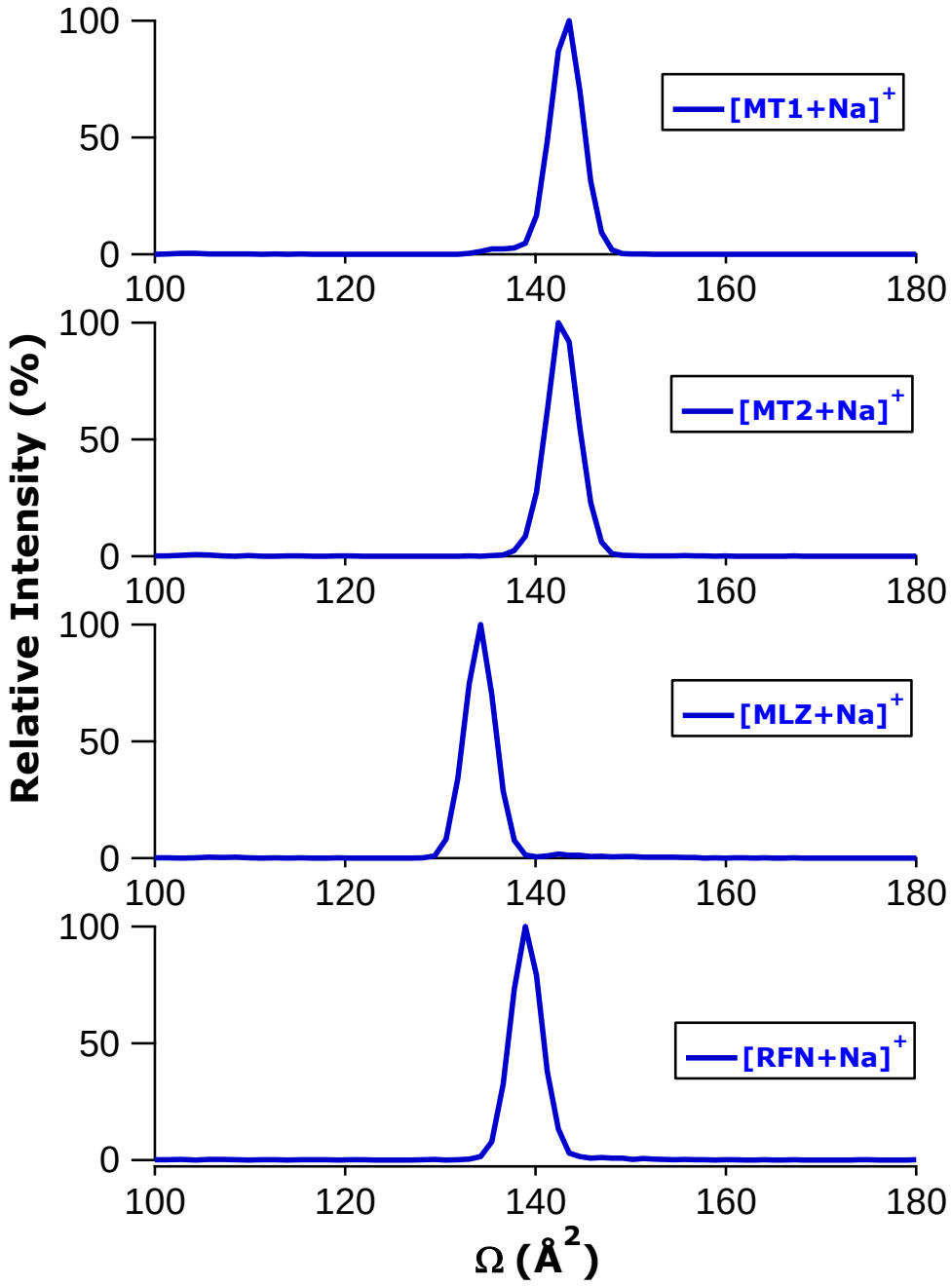

Figure S7. Representative distributions of ion-neutral CCS values for MT1, MT2, MLZ, and RFN as their sodium ion adducts.

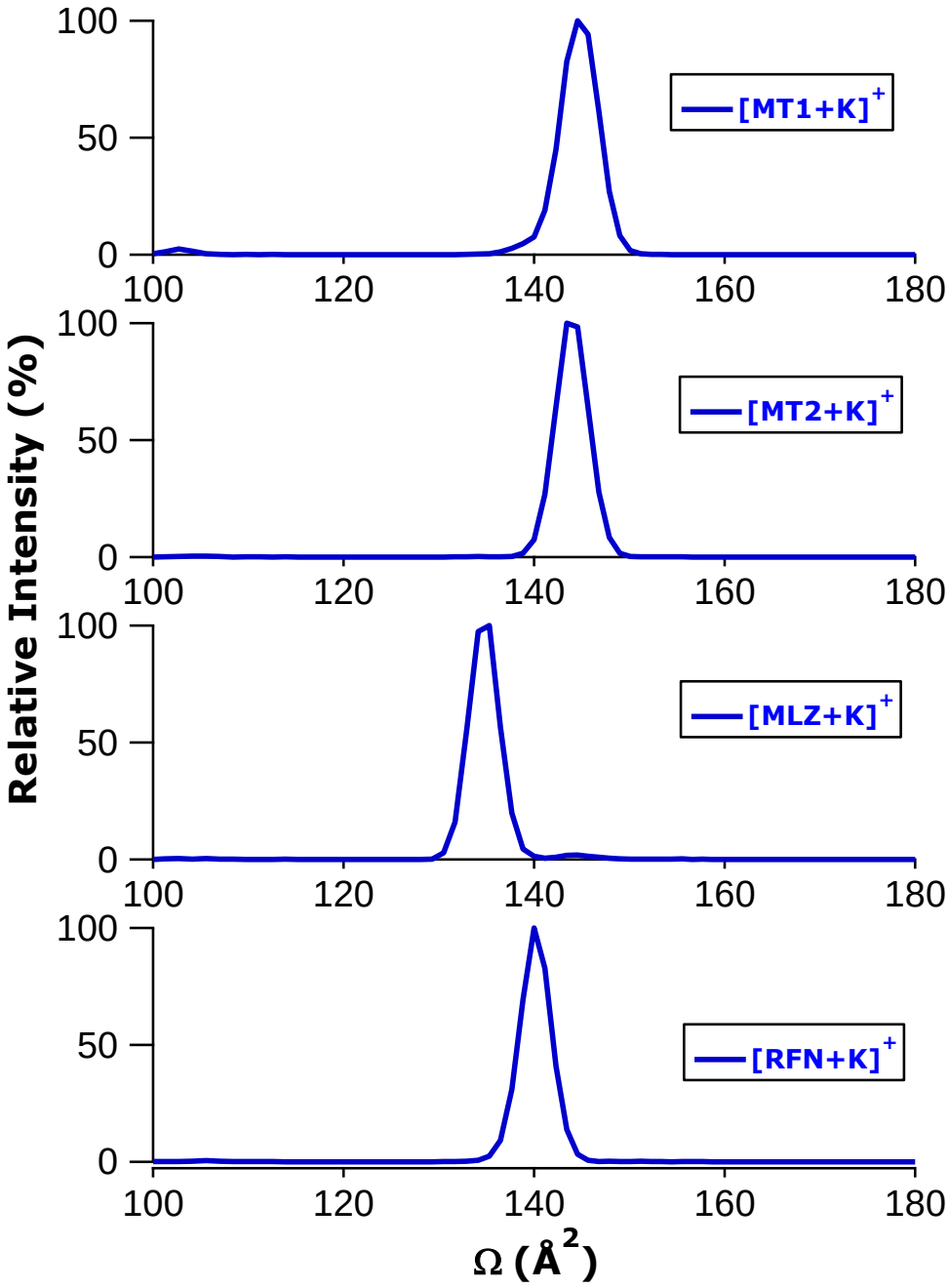

Figure S8. Representative distributions of ion-neutral CCS values for MT1, MT2, MLZ, and RFN as their potassium ion adducts.

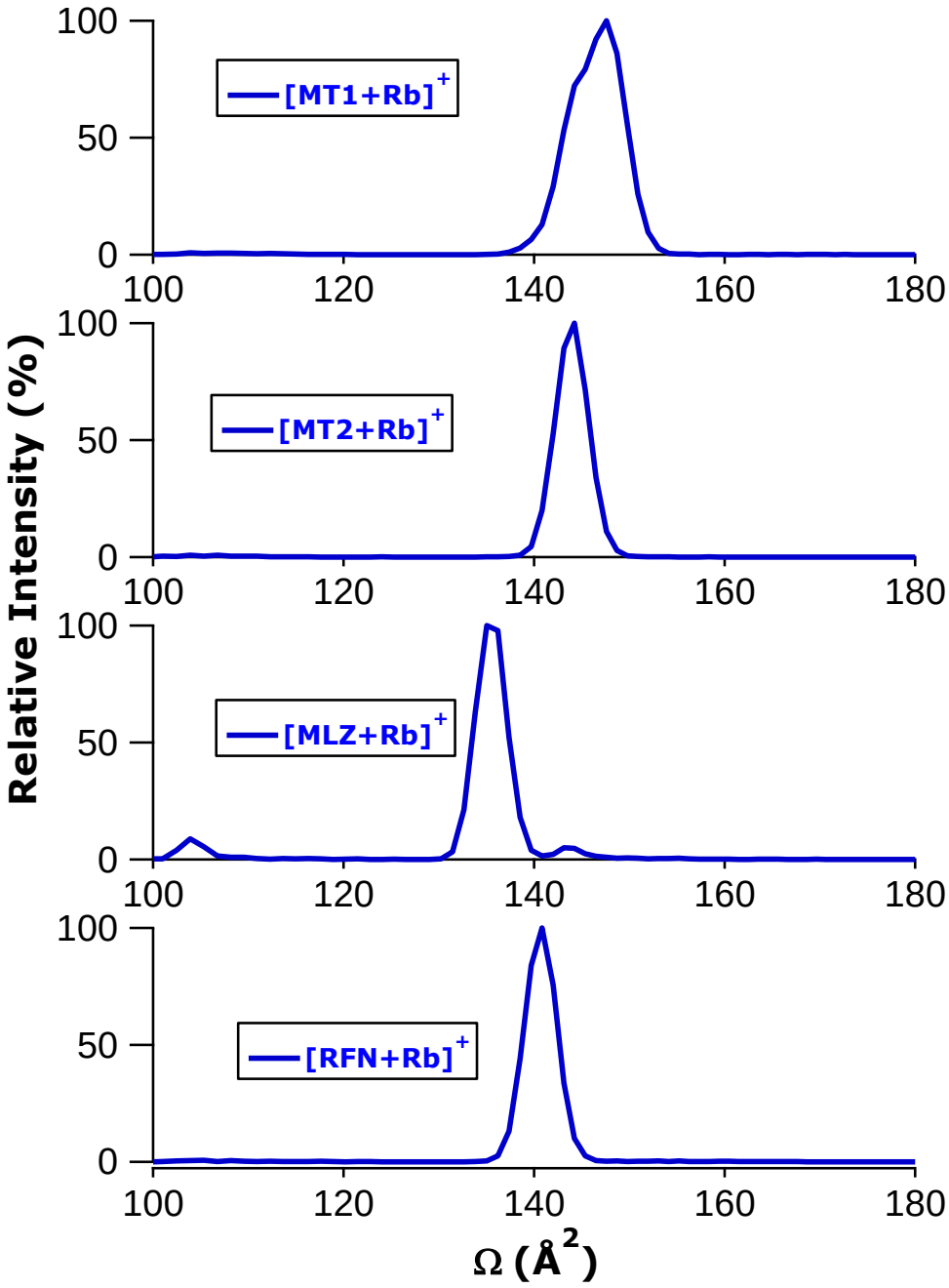

Figure S9. Representative distributions of ion-neutral CCS values for MT1, MT2, MLZ, and RFN as their rubidium ion adducts.

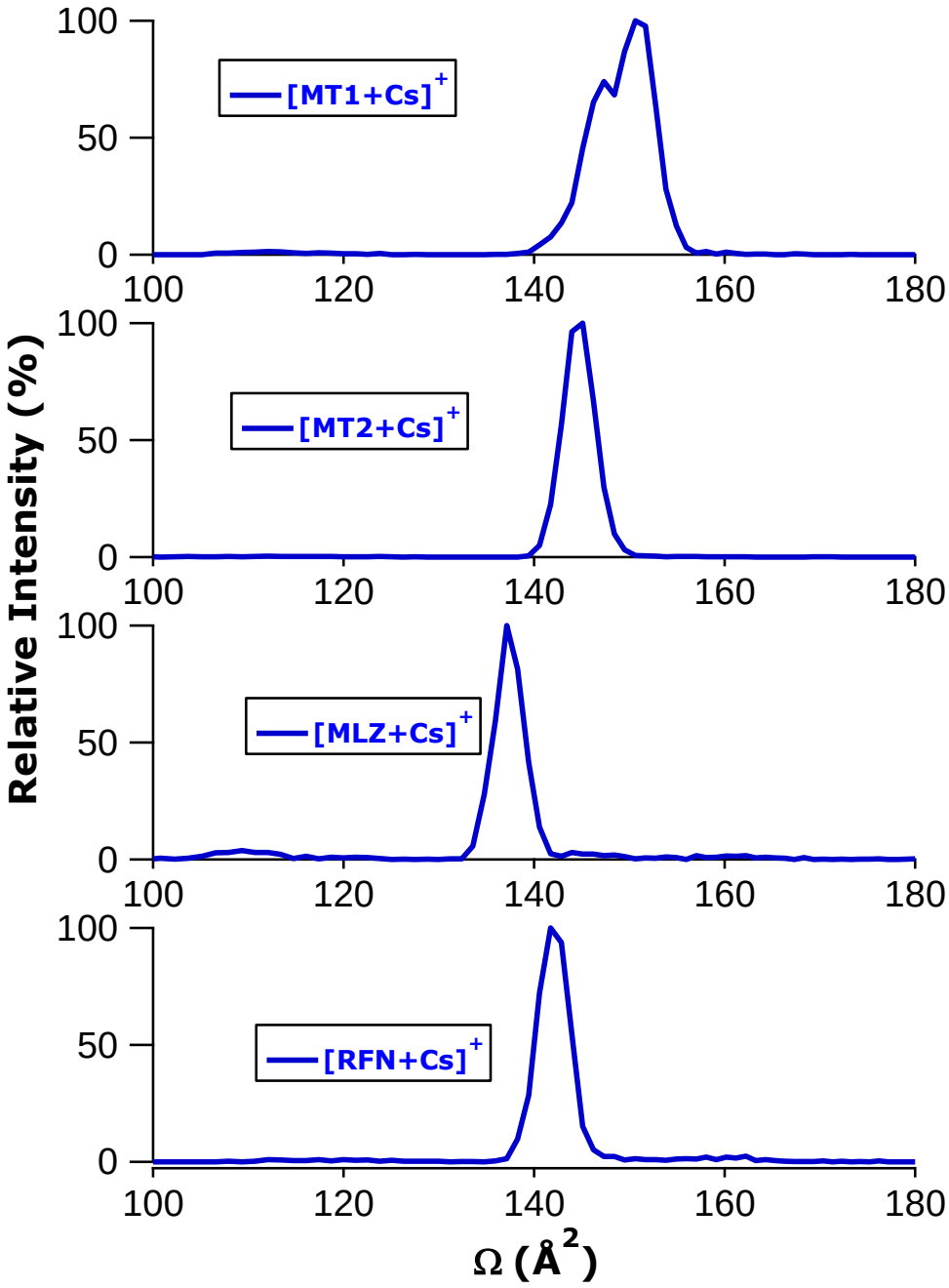

Figure S10. Representative distributions of ion-neutral CCS values for MT1, MT2, MLZ, and RFN as their cesium ion adducts.

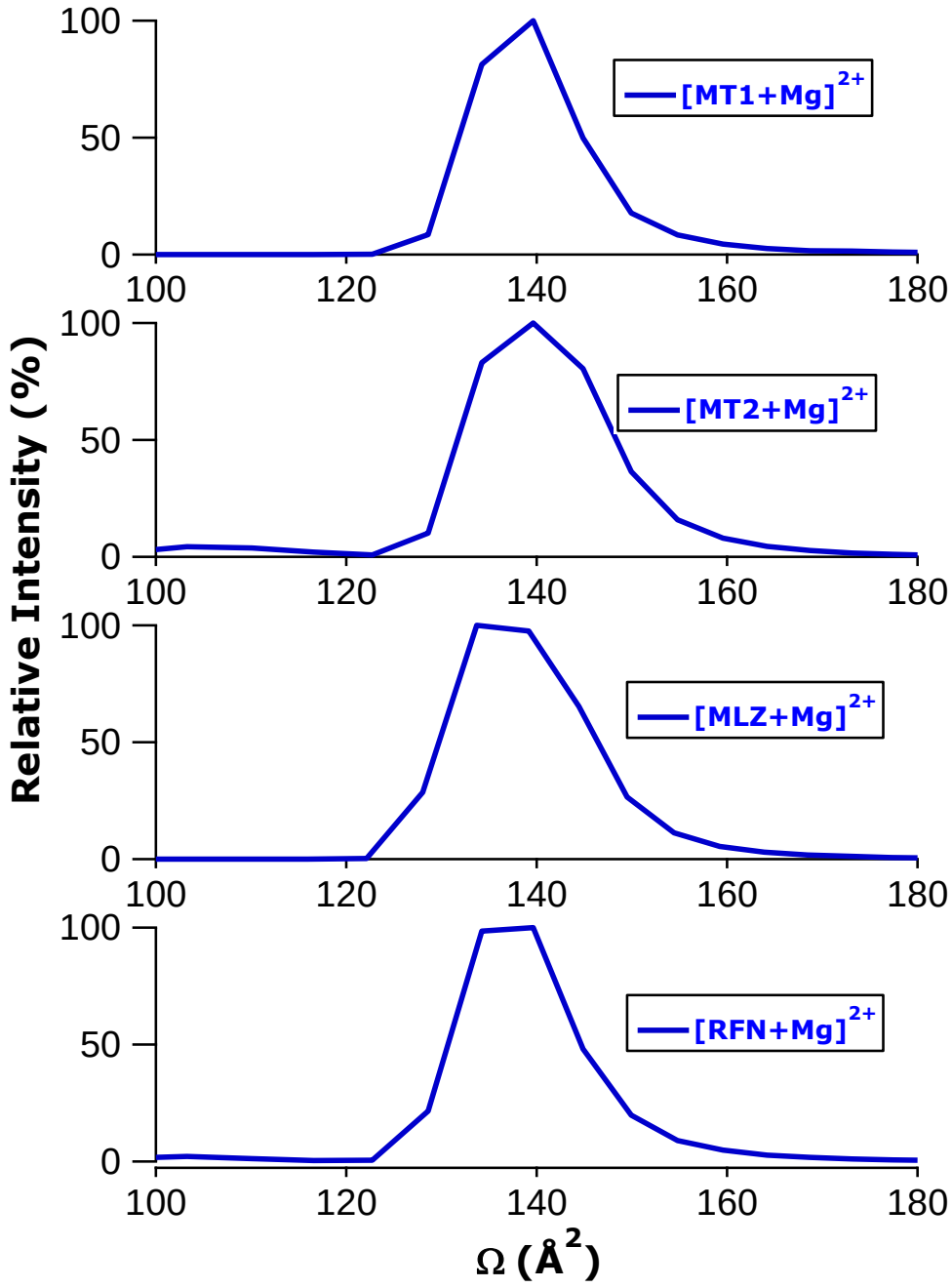

Figure S11. Representative distributions of ion-neutral CCS values for MT1, MT2, MLZ, and RFN as their magnesium ion adducts.

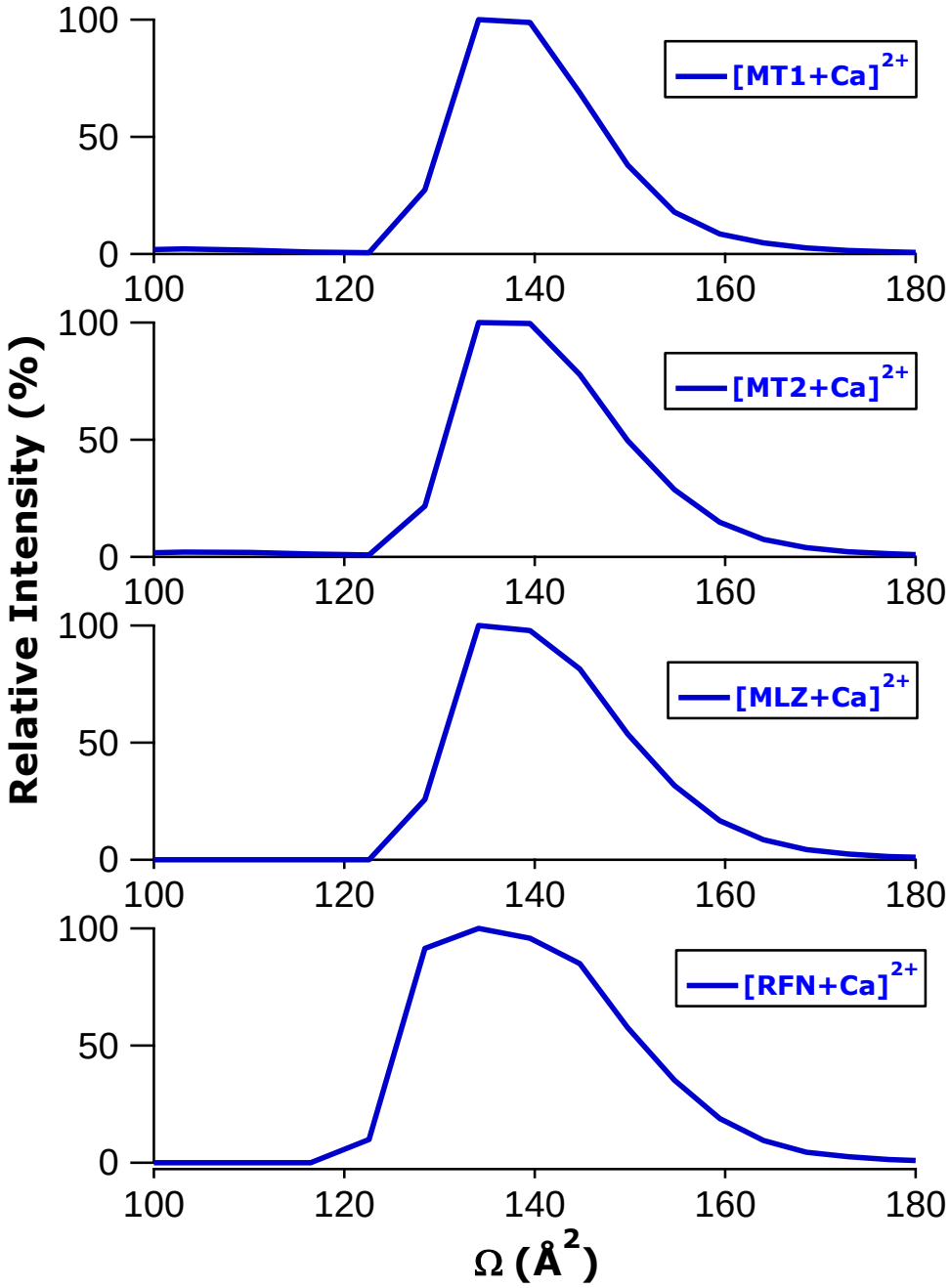

Figure S12. Representative distributions of ion-neutral CCS values for MT1, MT2, MLZ, and RFN as their calcium ion adducts.

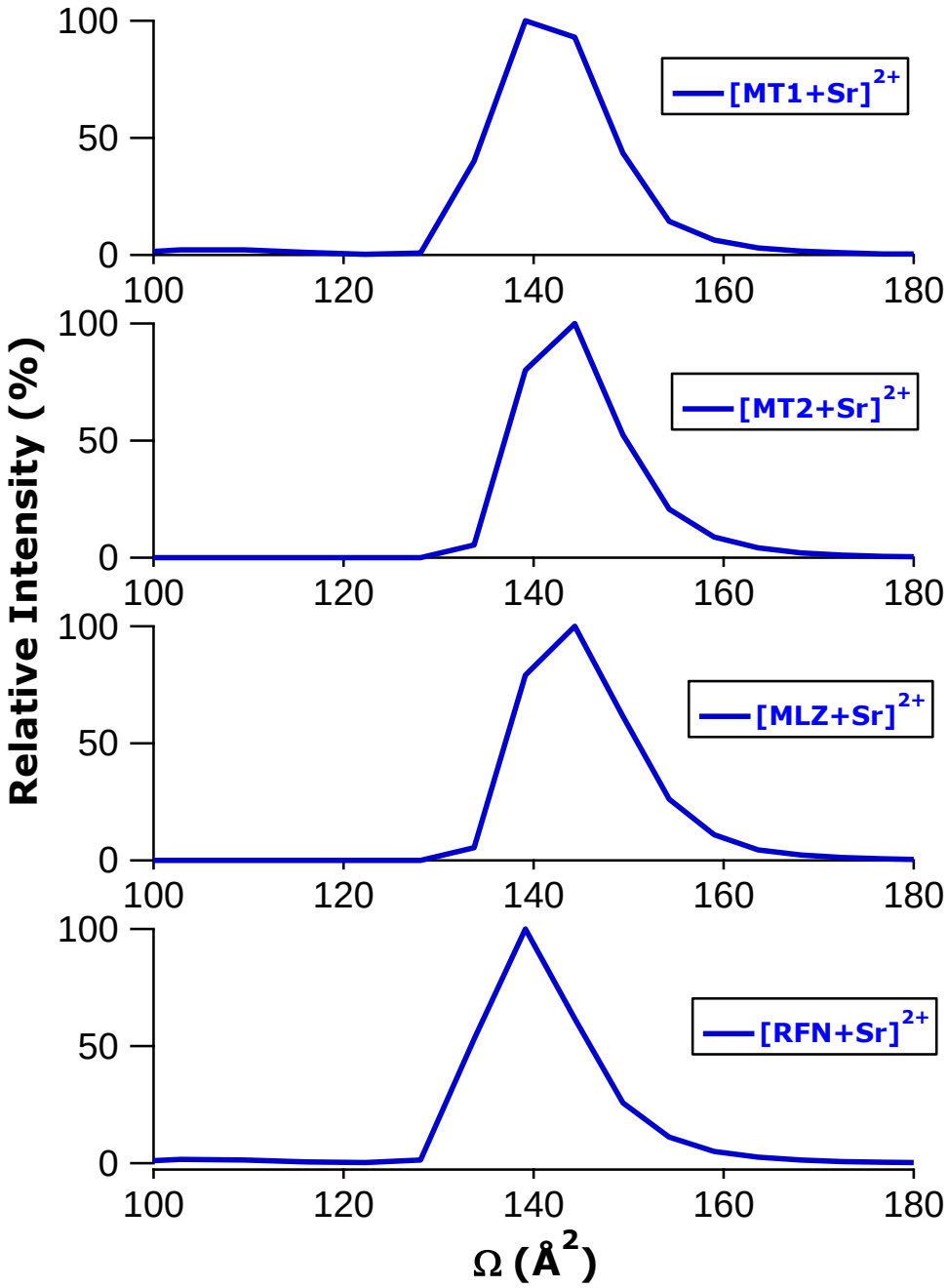

Figure S13. Representative distributions of ion-neutral CCS values for MT1, MT2, MLZ, and RFN as their strontium ion adducts.

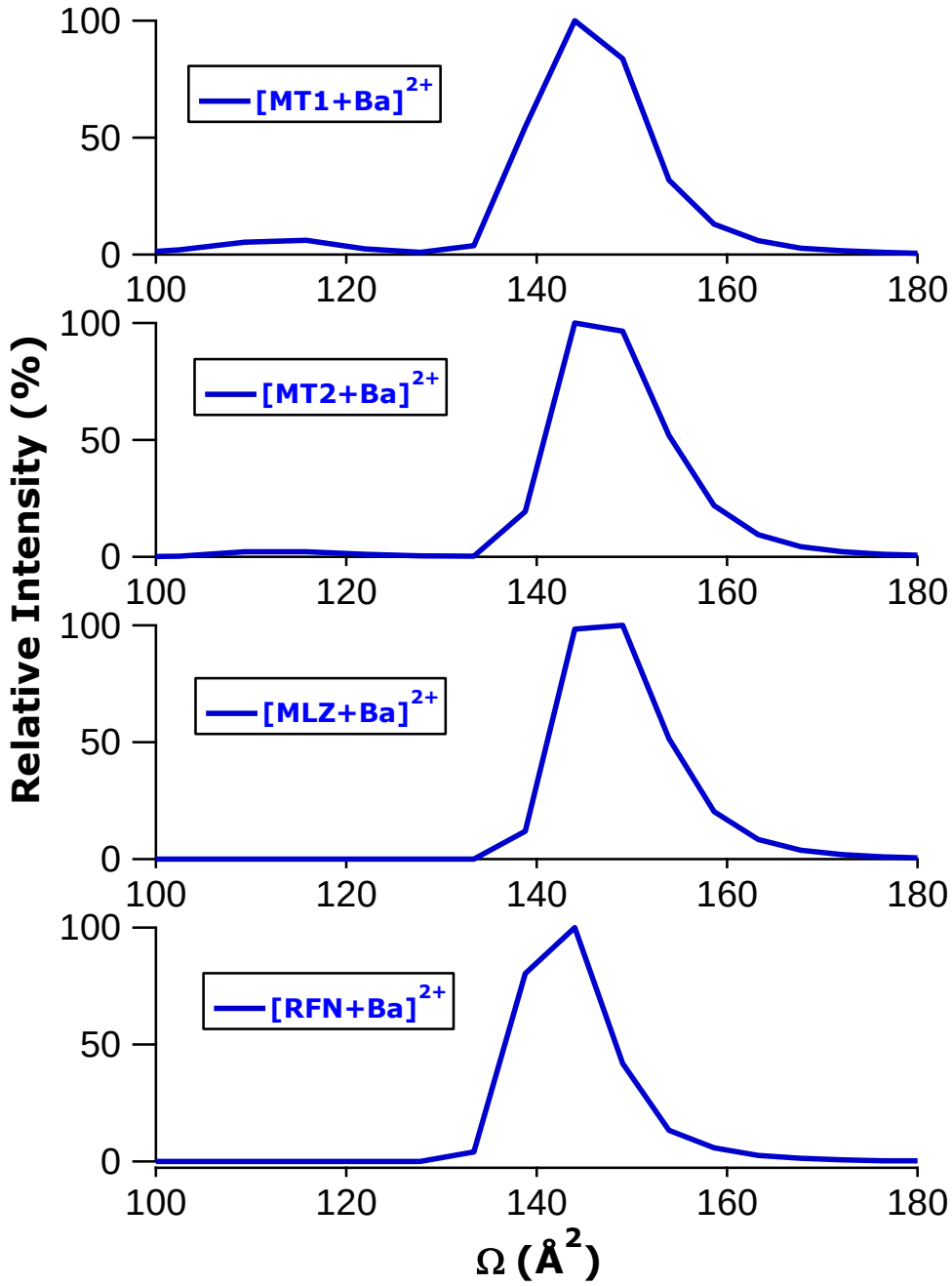

Figure S14. Representative distributions of ion-neutral CCS values for MT1, MT2, MLZ, and RFN as their barium ion adducts.

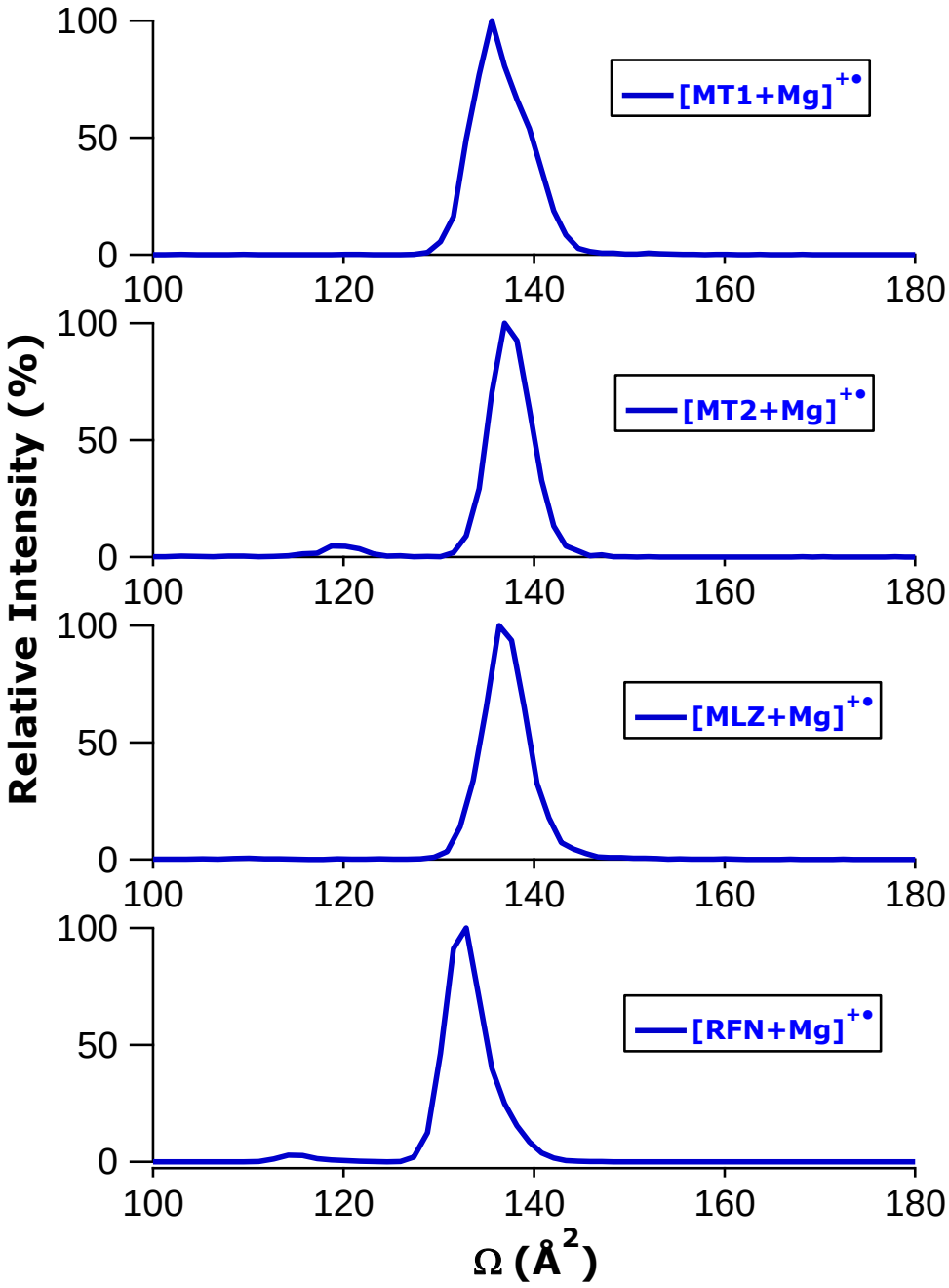

Figure S15. Representative distributions of ion-neutral CCS values for MT1, MT2, MLZ, and RFN as the ET products of their magnesium ion adducts.

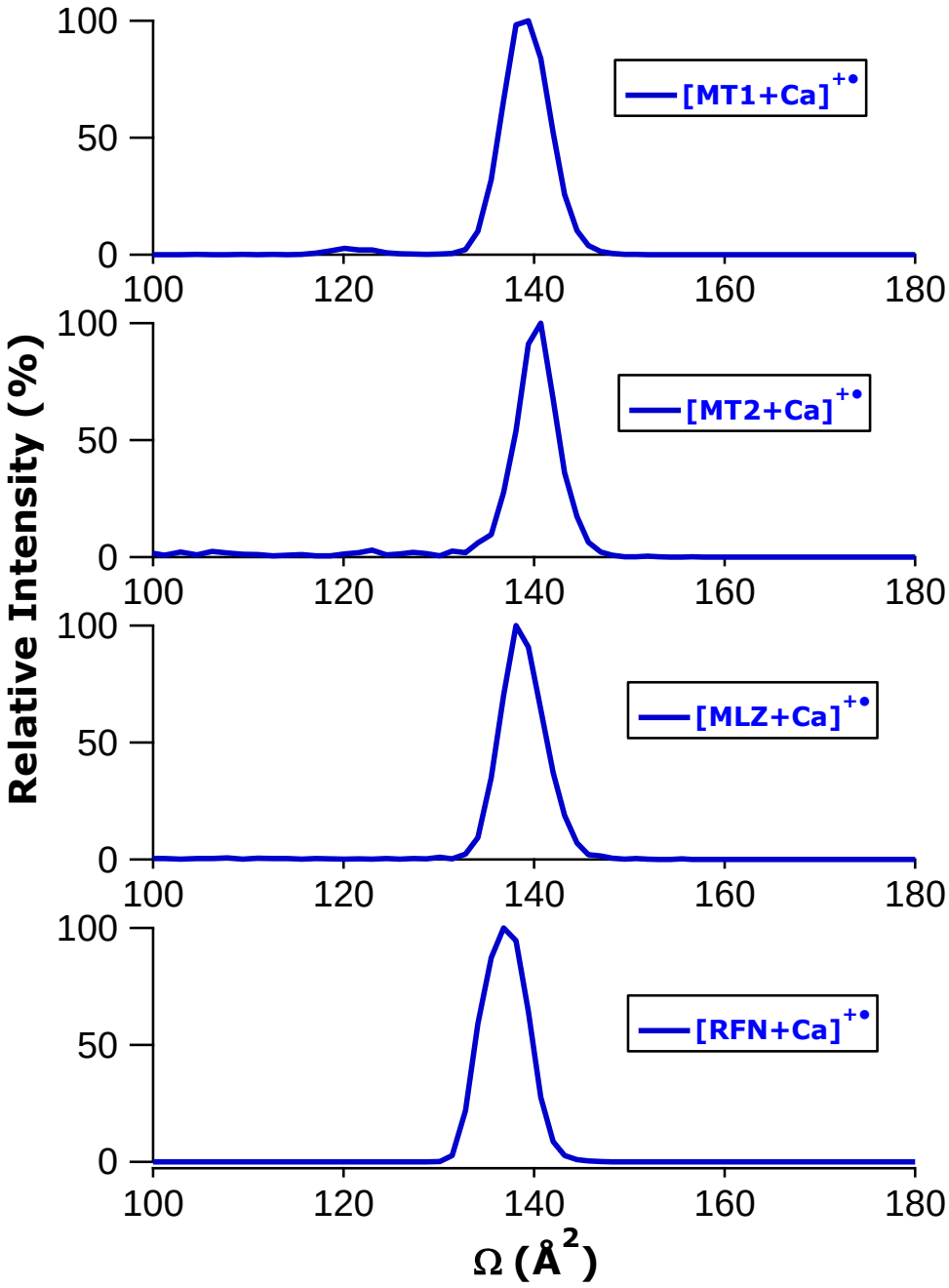

Figure S16. Representative distributions of ion-neutral CCS values for MT1, MT2, MLZ, and RFN as the ET products of their calcium ion adducts.

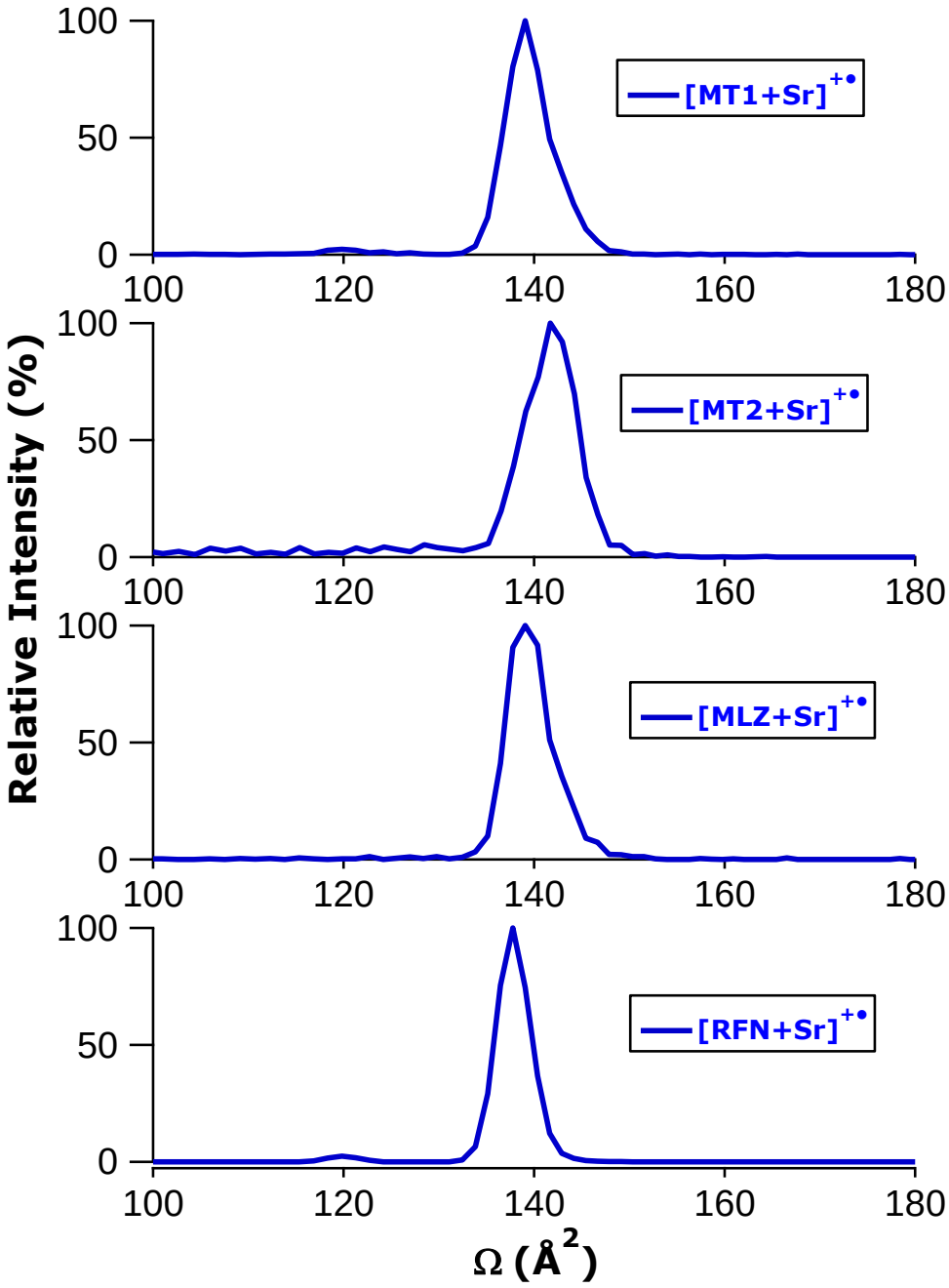

Figure S17. Representative distributions of ion-neutral CCS values for MT1, MT2, MLZ, and RFN as the ET products of their strontium ion adducts.

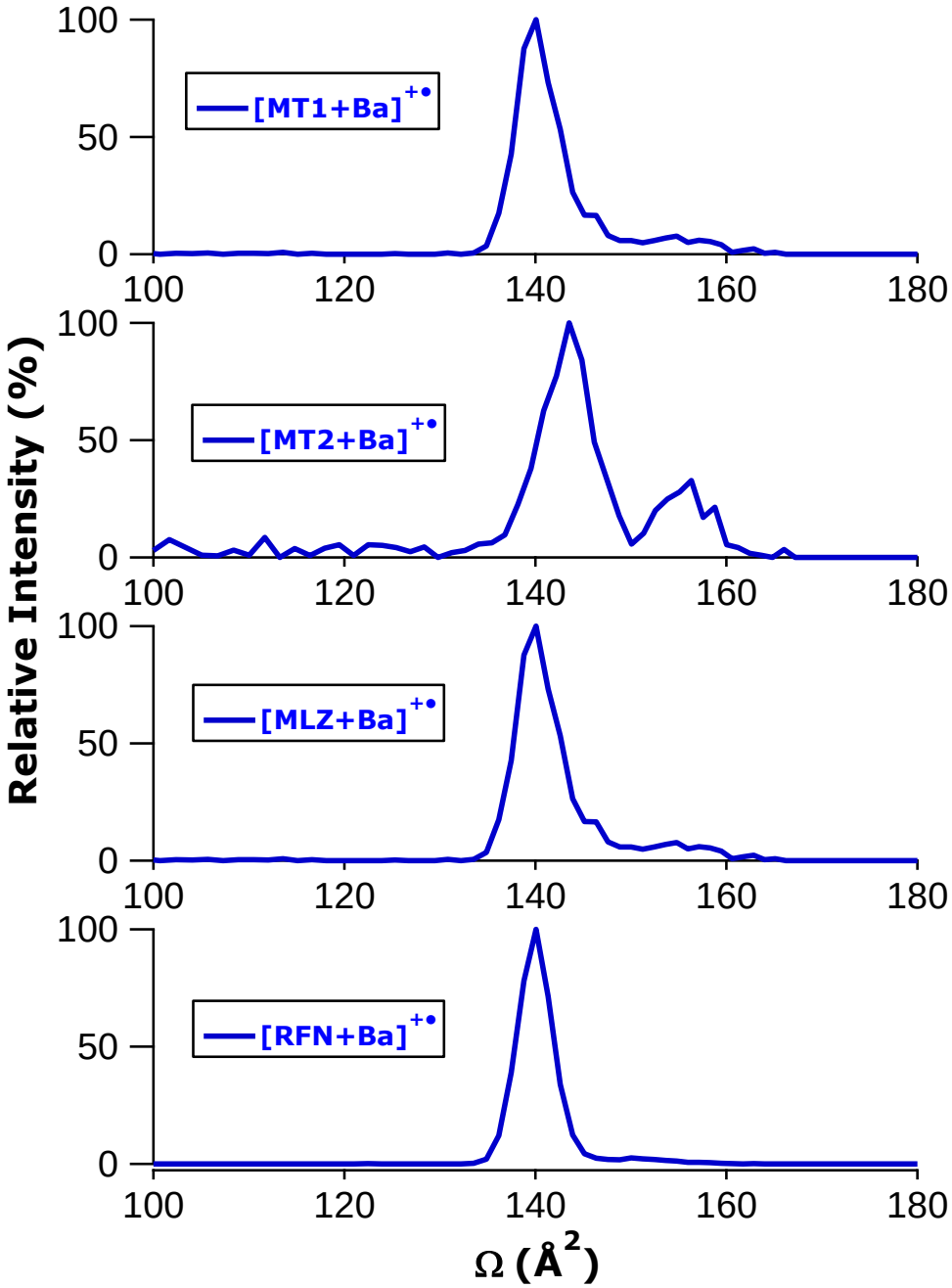

Figure S18. Representative distributions of ion-neutral CCS values for MT1, MT2, MLZ, and RFN as the ET products of their barium ion adducts.

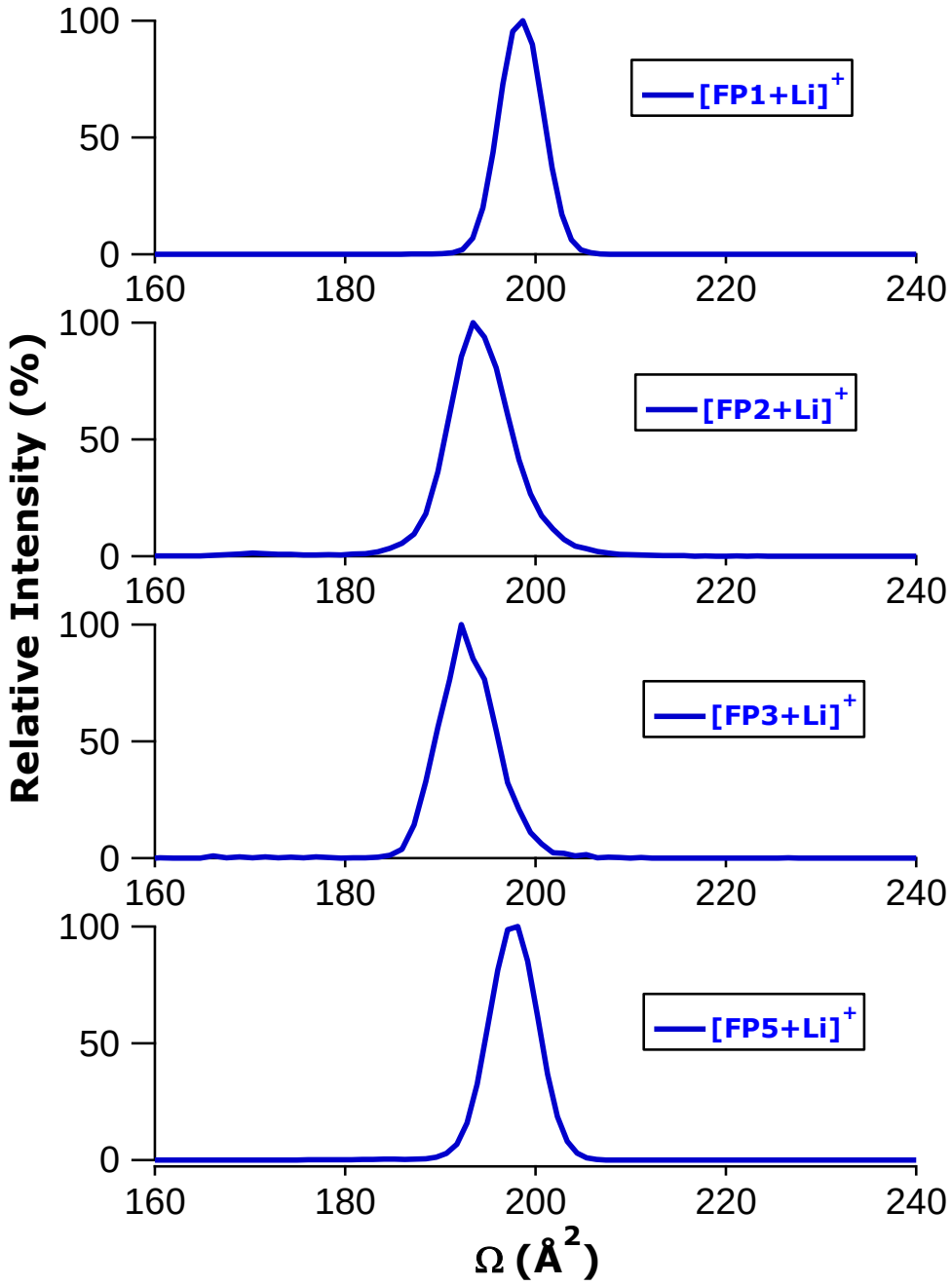

Figure S19. Representative distributions of ion-neutral CCS values for FP1, FP2, FP3, and FP5 as their lithium ion adducts.

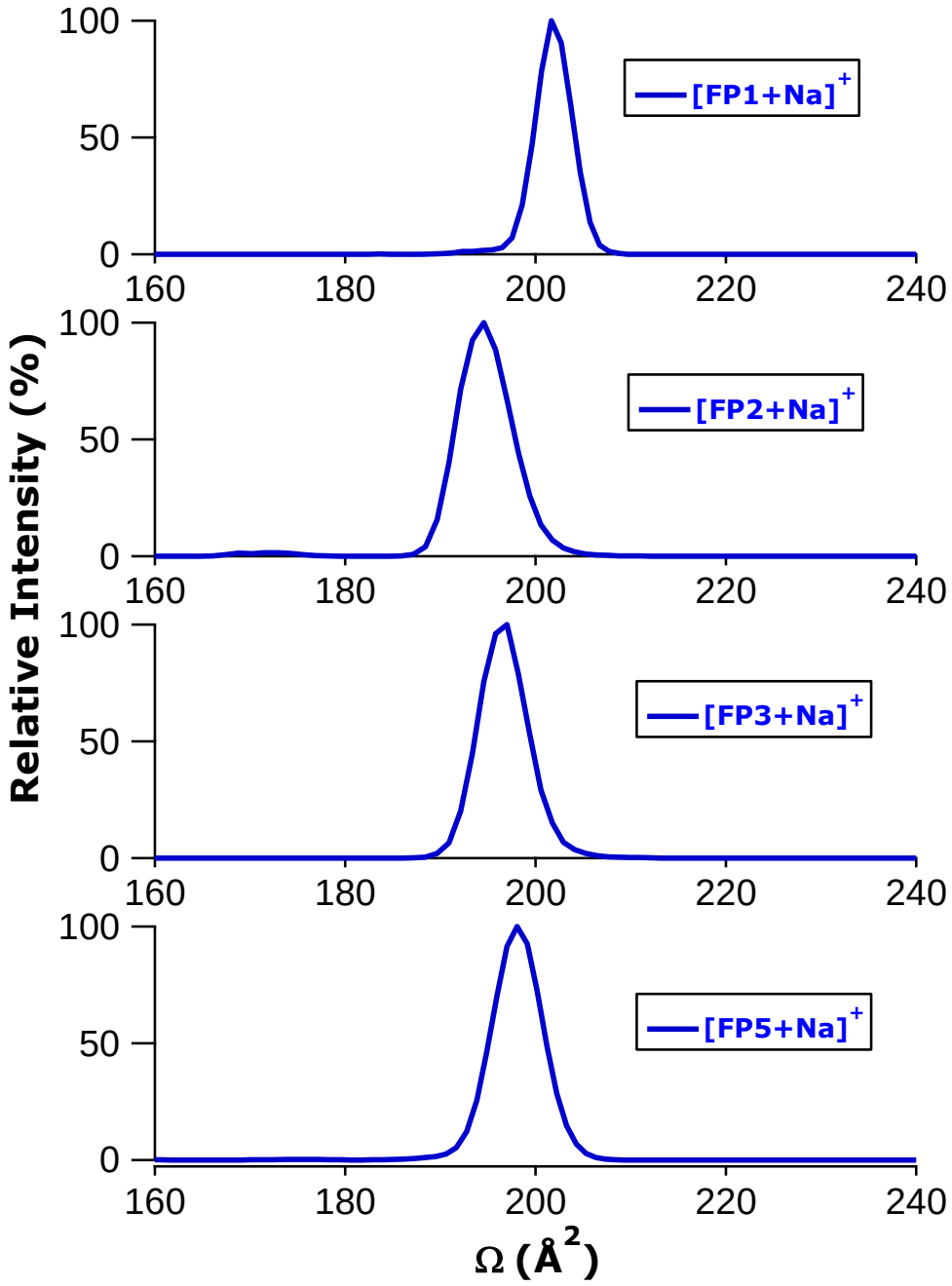

Figure S20. Representative distributions of ion-neutral CCS values for FP1, FP2, FP3, and FP5 as their sodium ion adducts.

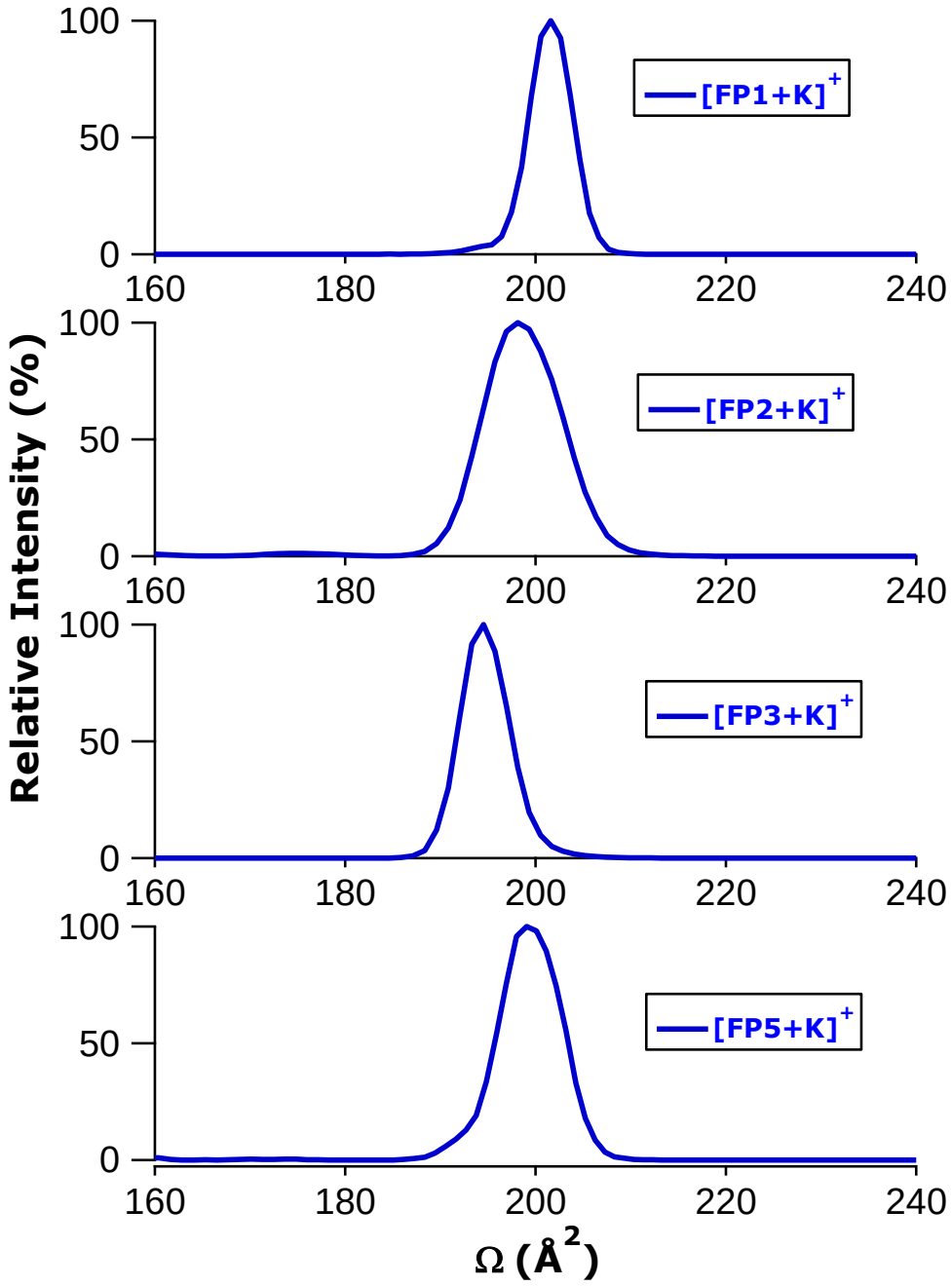

Figure S21. Representative distributions of ion-neutral CCS values for FP1, FP2, FP3, and FP5 as their potassium ion adducts.

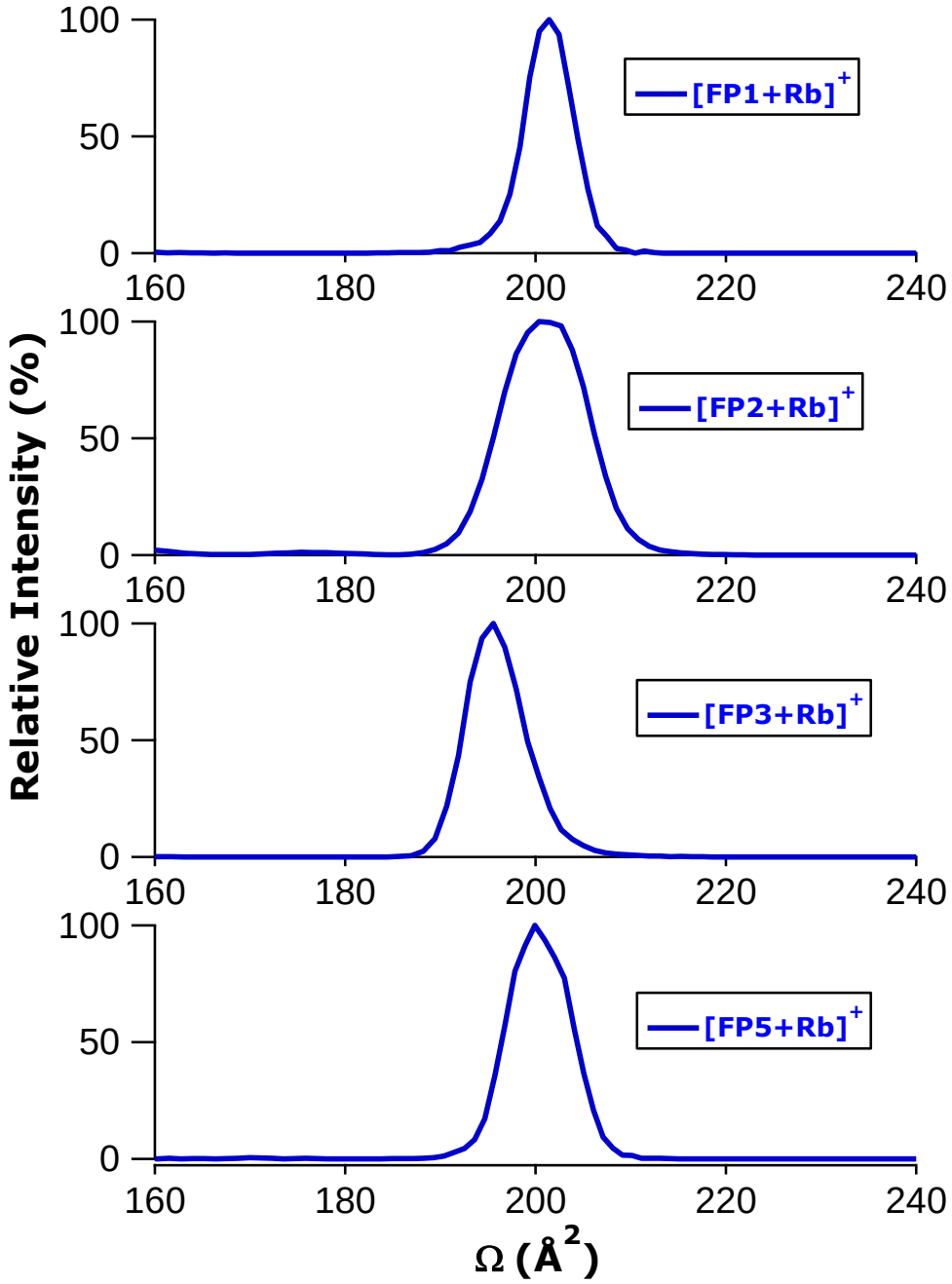

Figure S22. Representative distributions of ion-neutral CCS values for FP1, FP2, FP3, and FP5 as their rubidium ion adducts.

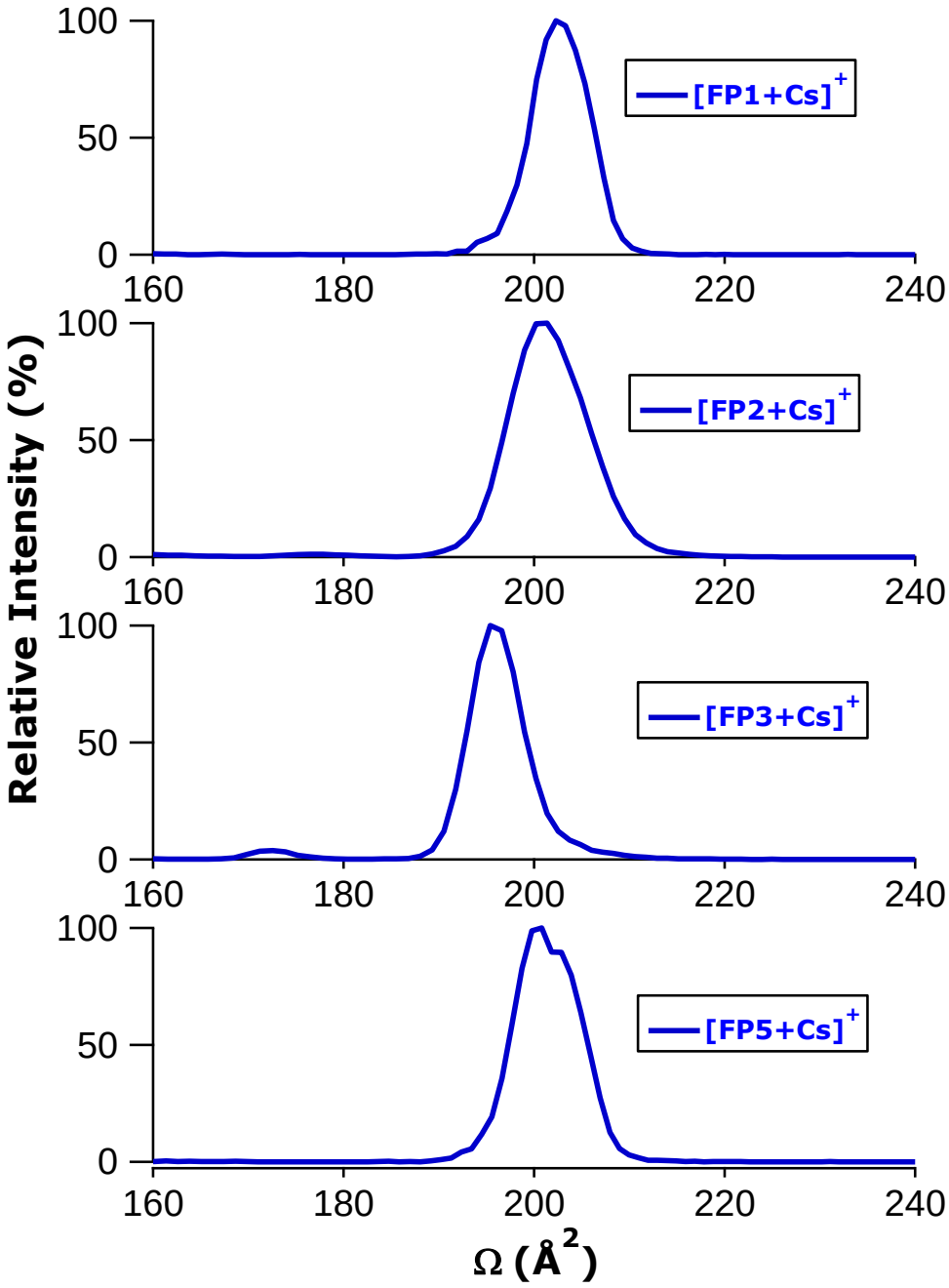

Figure S23. Representative distributions of ion-neutral CCS values for FP1, FP2, FP3, and FP5 as their cesium ion adducts.

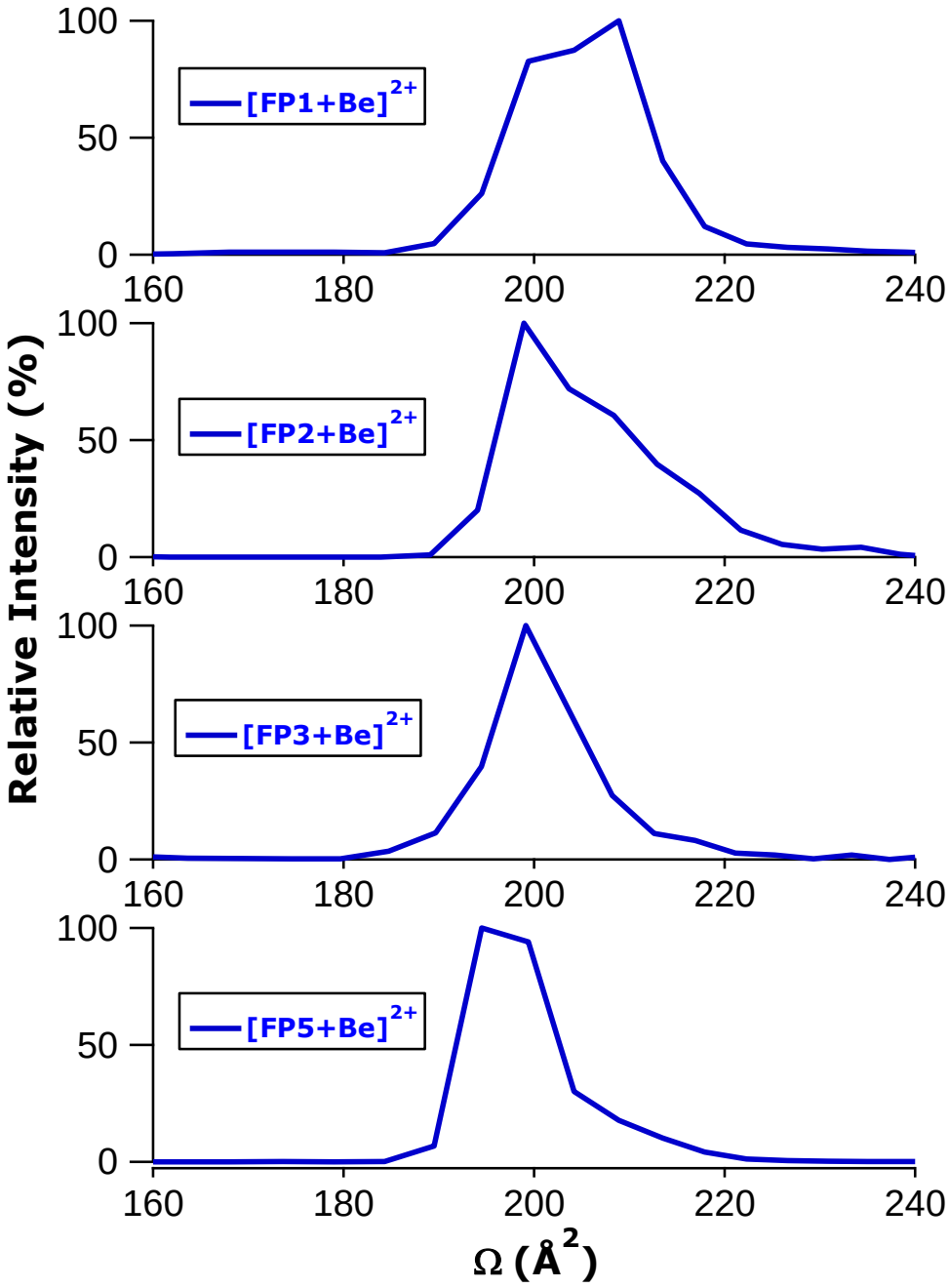

Figure S24. Representative distributions of ion-neutral CCS values for FP1, FP2, FP3, and FP5 as their beryllium ion adducts.

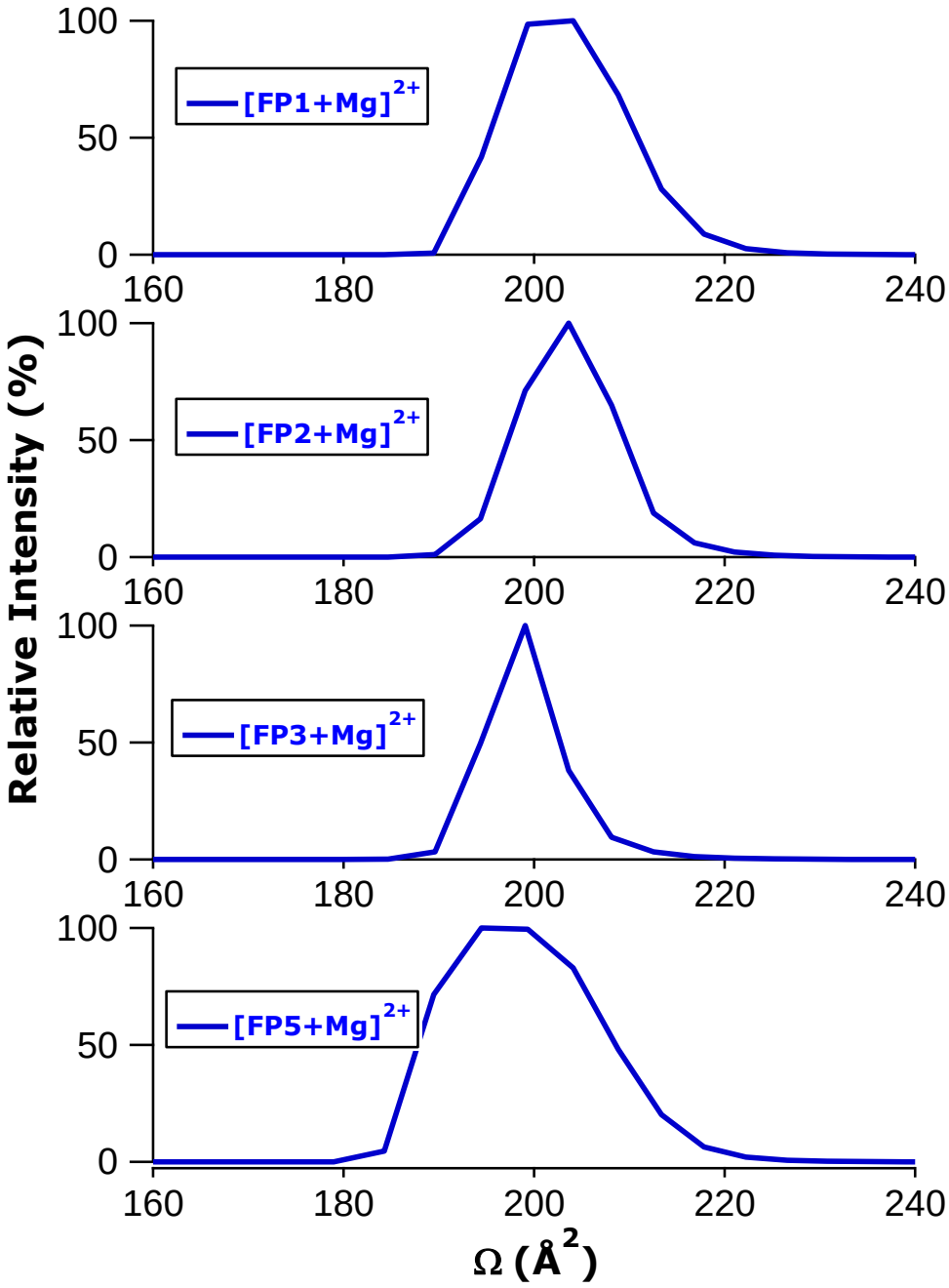

Figure S25. Representative distributions of ion-neutral CCS values for FP1, FP2, FP3, and FP5 as their magnesium ion adducts.

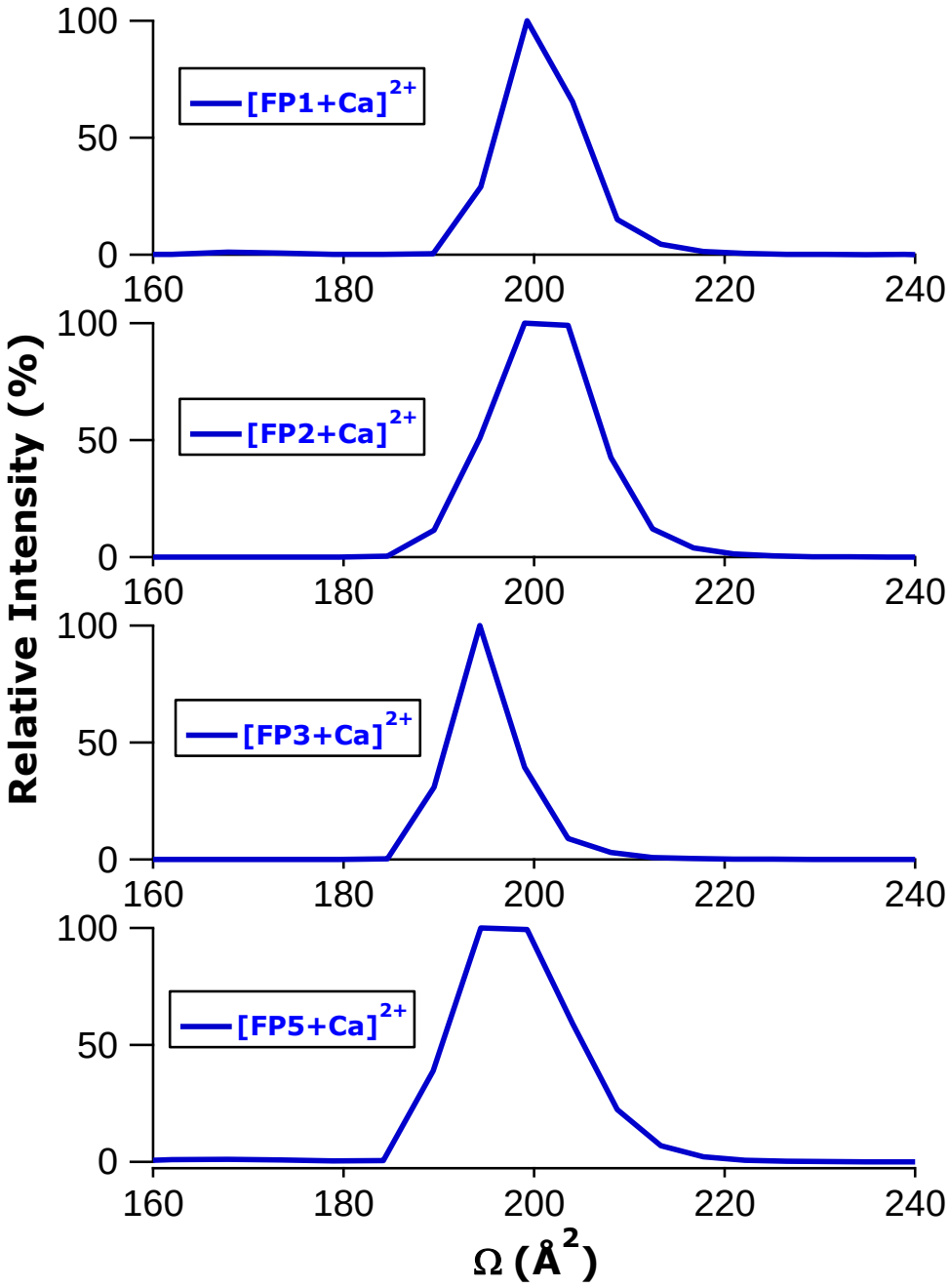

Figure S26. Representative distributions of ion-neutral CCS values for FP1, FP2, FP3, and FP5 as their calcium ion adducts.

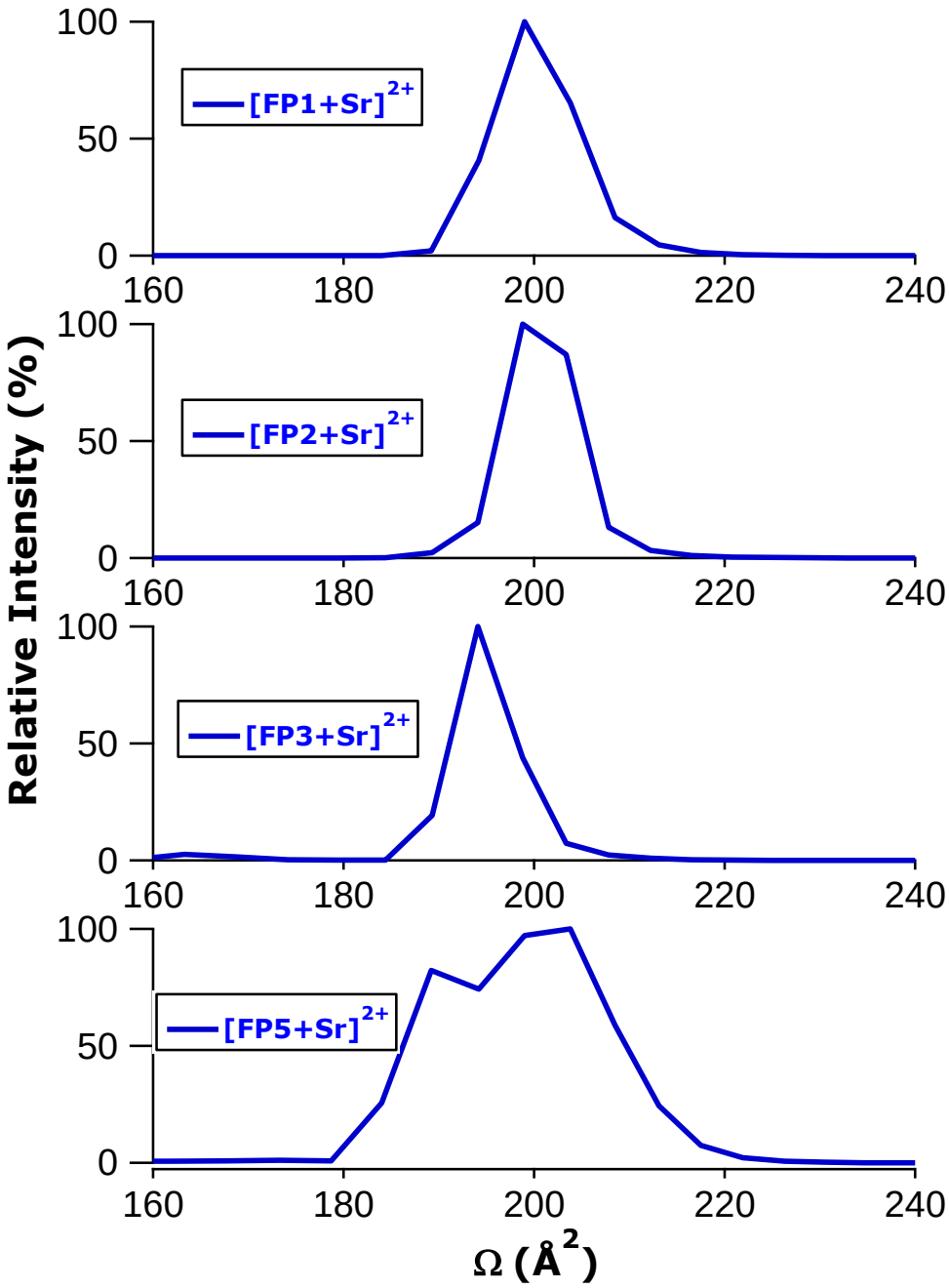

Figure S27. Representative distributions of ion-neutral CCS values for FP1, FP2, FP3, and FP5 as their strontium ion adducts.

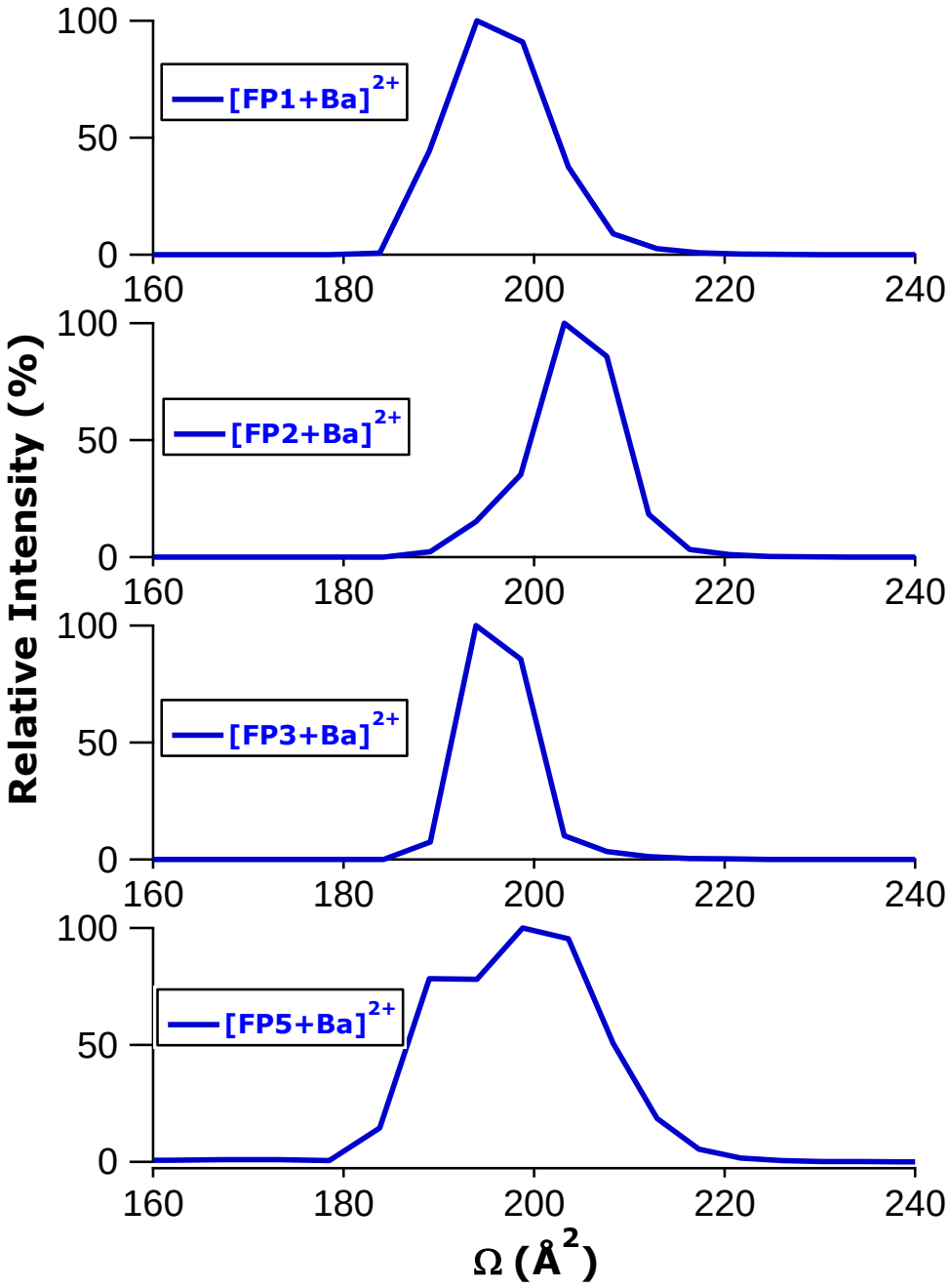

Figure S28. Representative distributions of ion-neutral CCS values for FP1, FP2, FP3, and FP5 as their barium ion adducts.

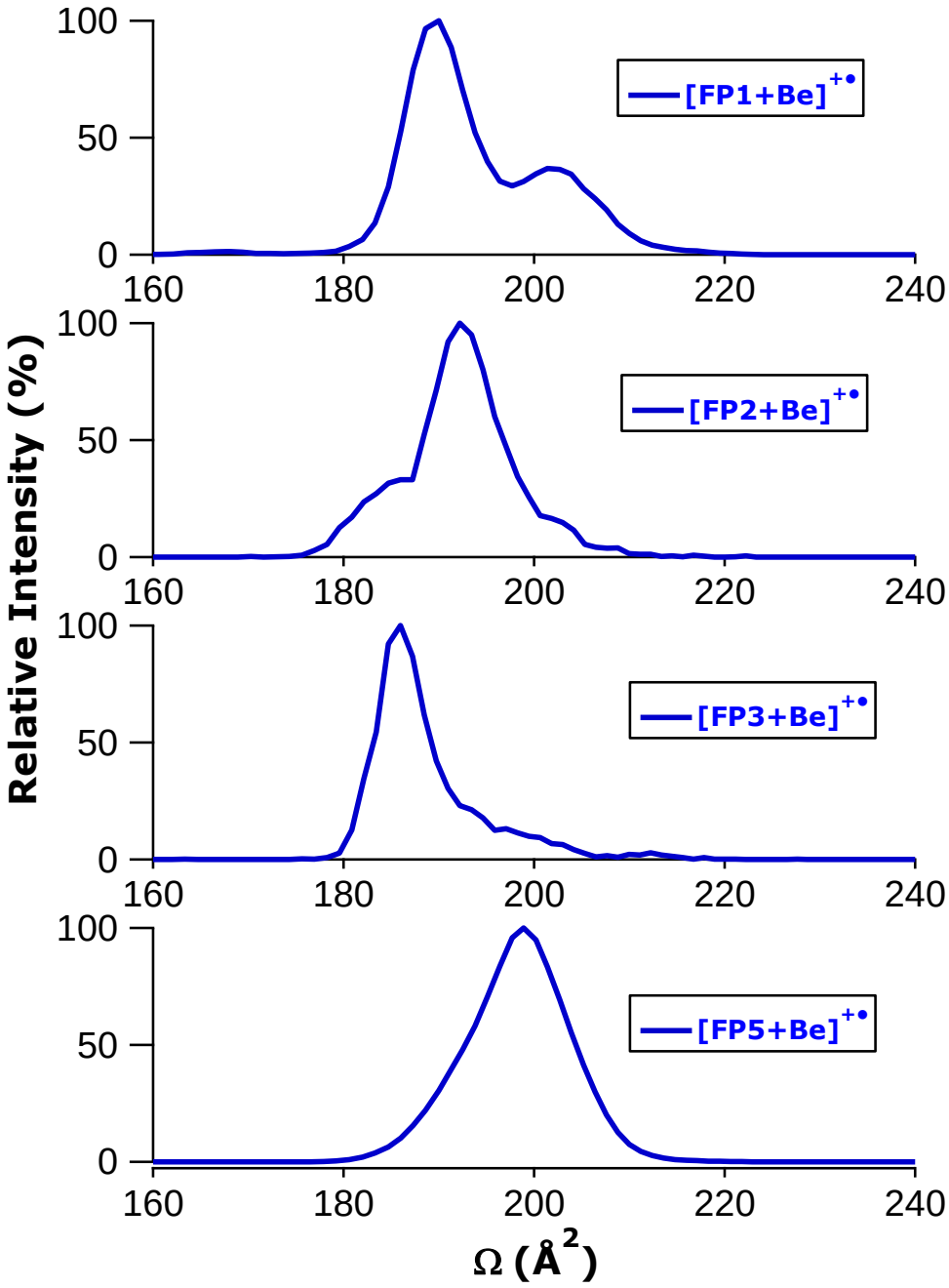

Figure S29. Representative distributions of ion-neutral CCS values for FP1, FP2, FP3, and FP5 as the ET products of their beryllium ion adducts.

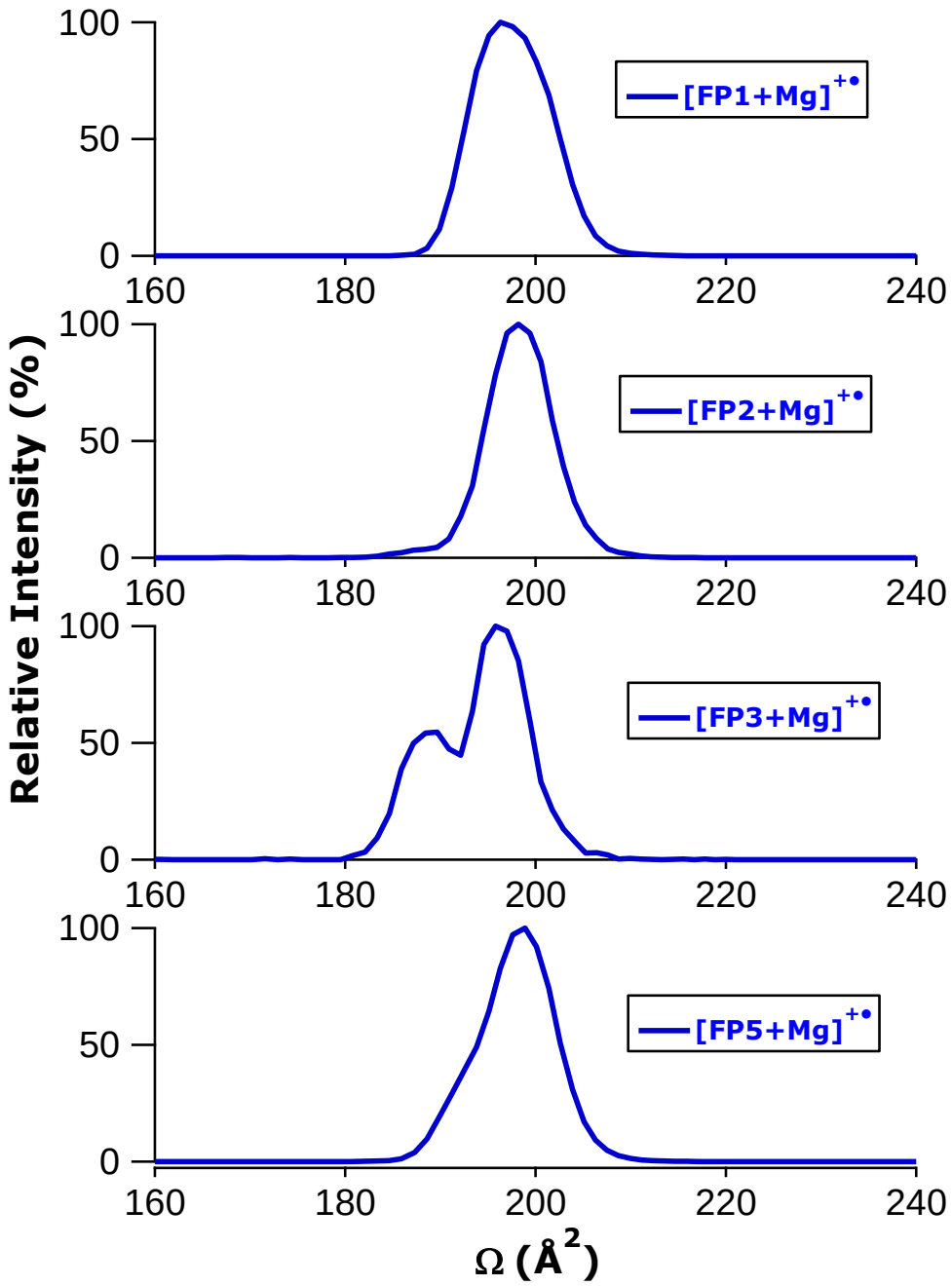

Figure S30. Representative distributions of ion-neutral CCS values for FP1, FP2, FP3, and FP5 as the ET products of their magnesium ion adducts.

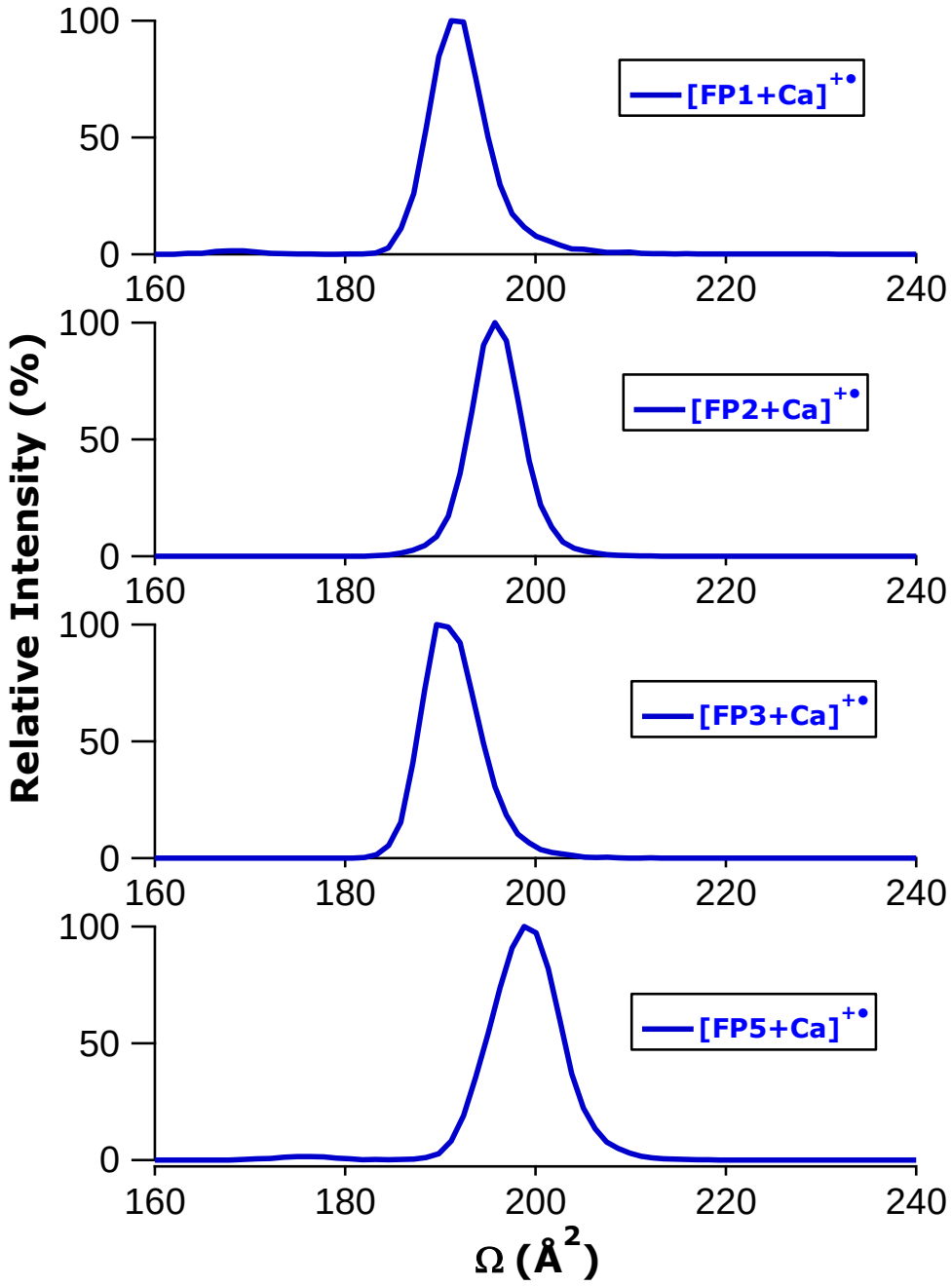

Figure S31. Representative distributions of ion-neutral CCS values for FP1, FP2, FP3, and FP5 as the ET products of their calcium ion adducts.

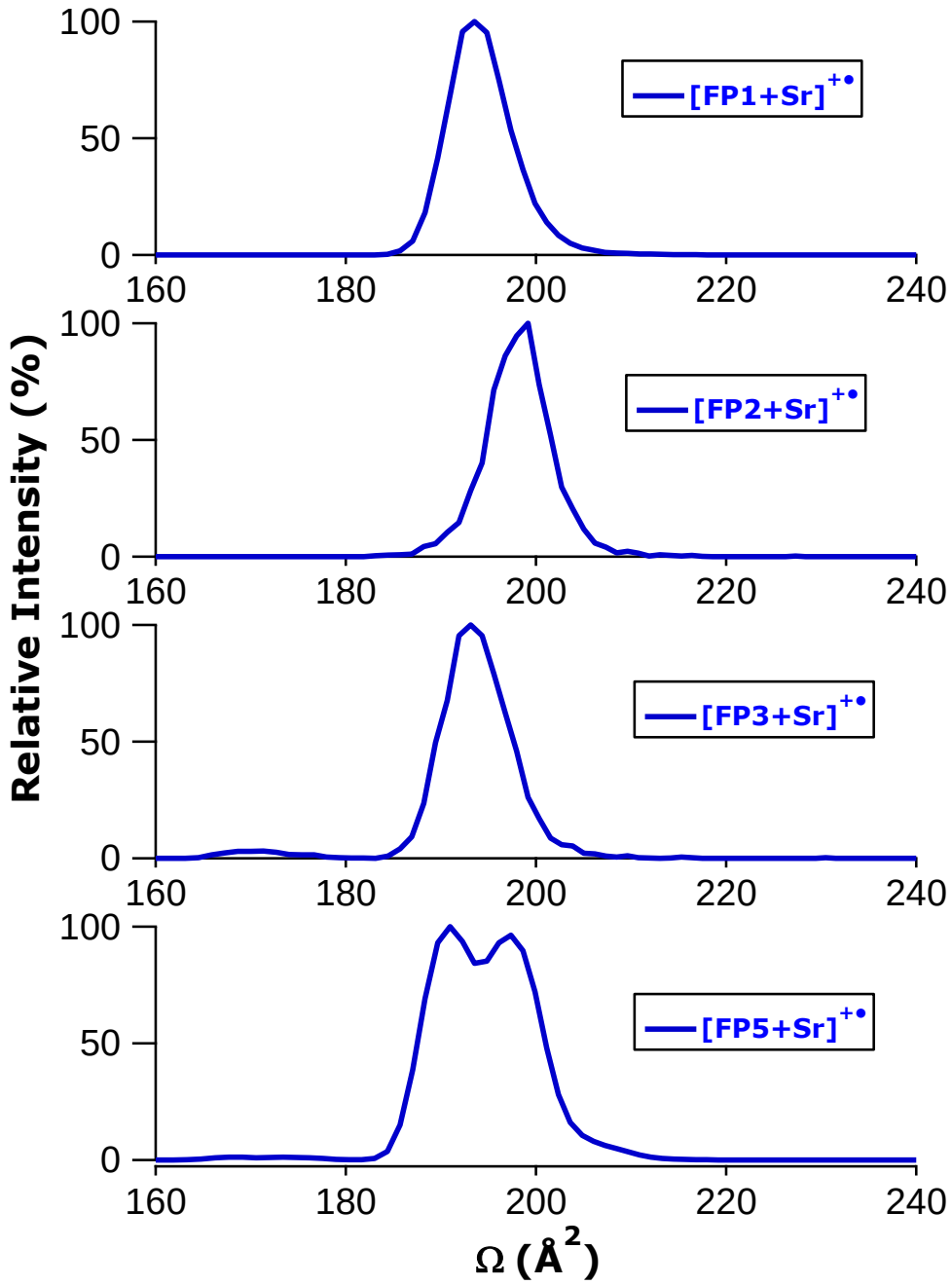

Figure S32. Representative distributions of ion-neutral CCS values for FP1, FP2, FP3, and FP5 as the ET products of their strontium ion adducts.

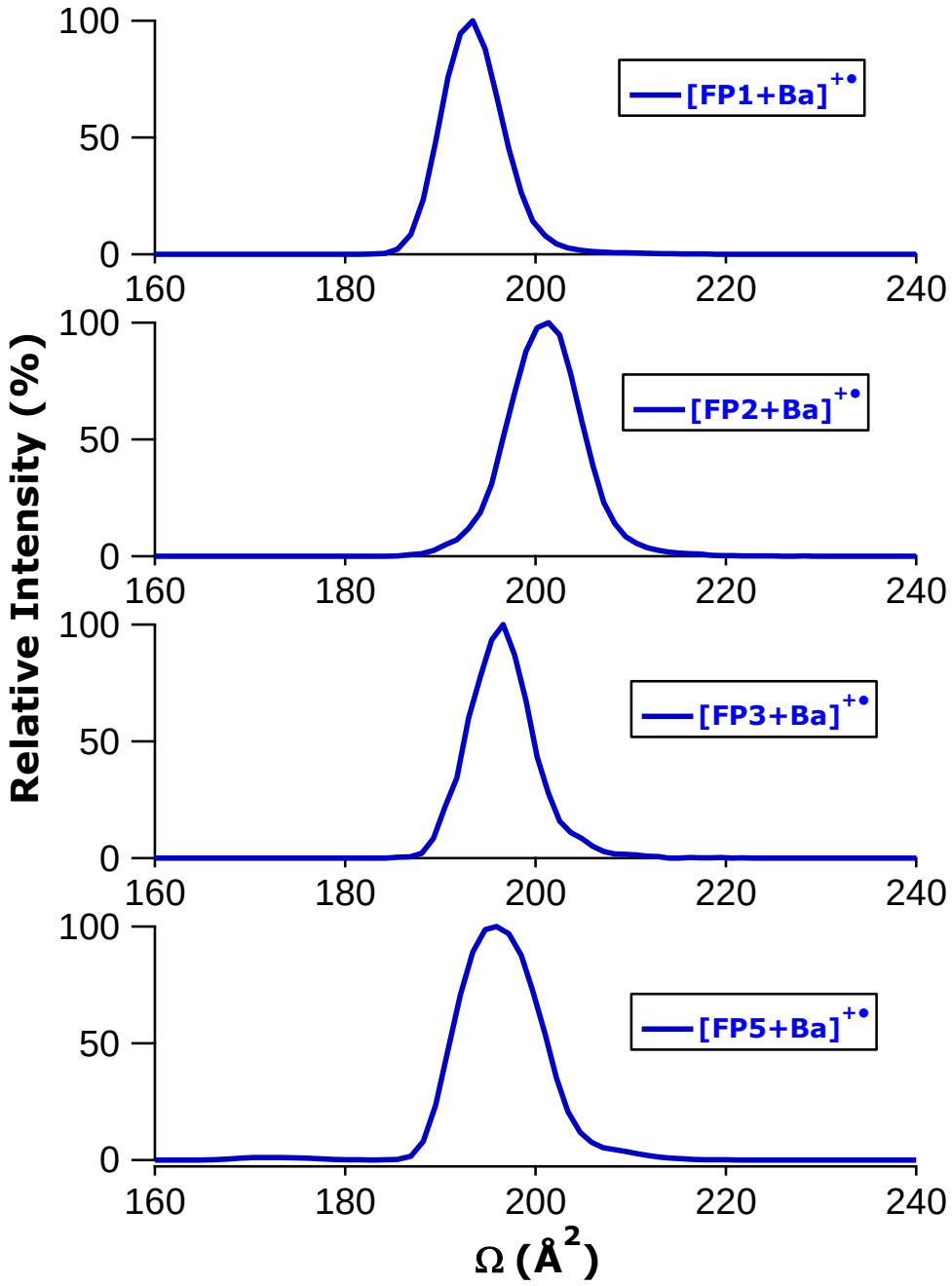

Figure S33. Representative distributions of ion-neutral CCS values for FP1, FP2, FP3, and FP5 as the ET products of their barium ion adducts.

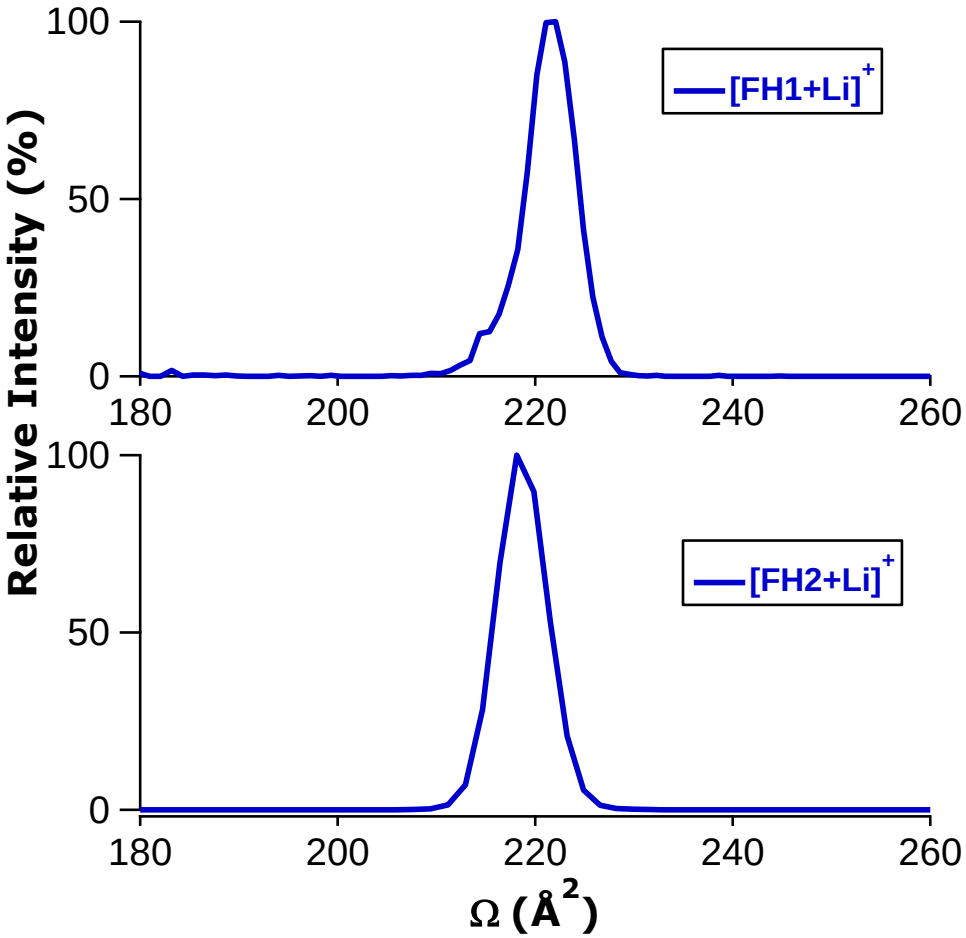

Figure S34. Representative distributions of ion-neutral CCS values for FH1 and FH2 as their lithium ion adducts.

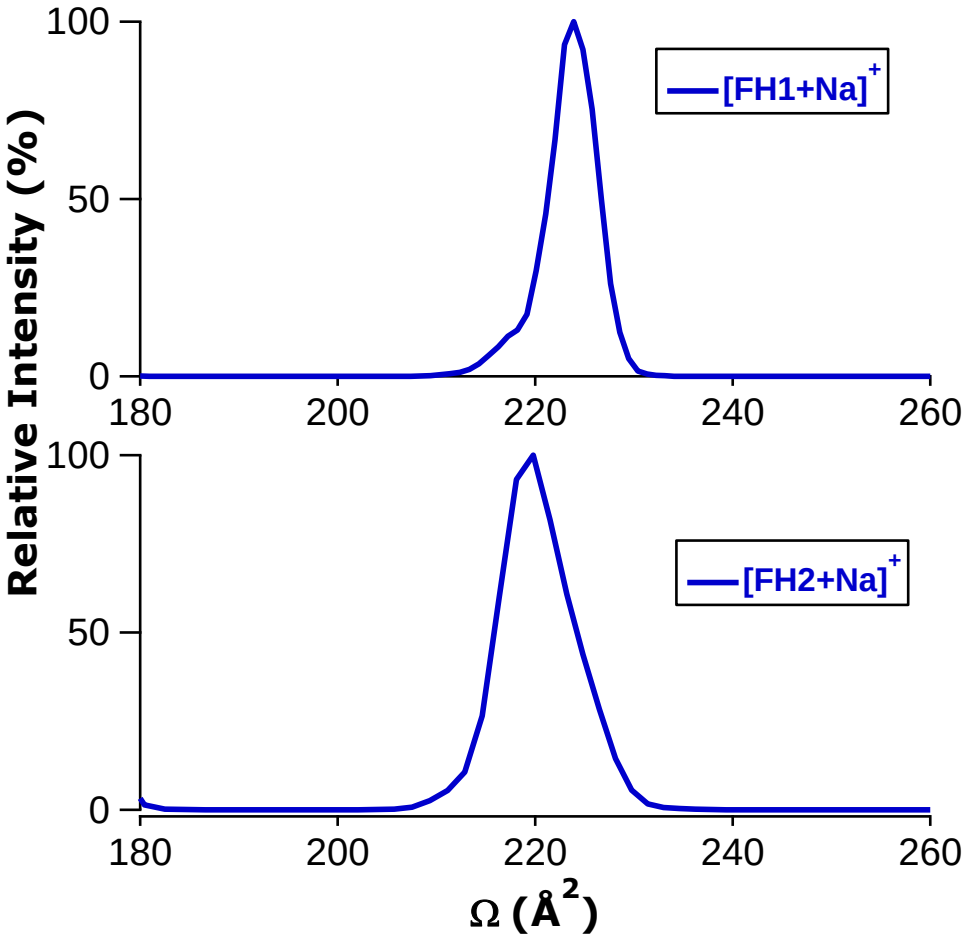

Figure S35. Representative distributions of ion-neutral CCS values for FH1 and FH2 as their sodium ion adducts.

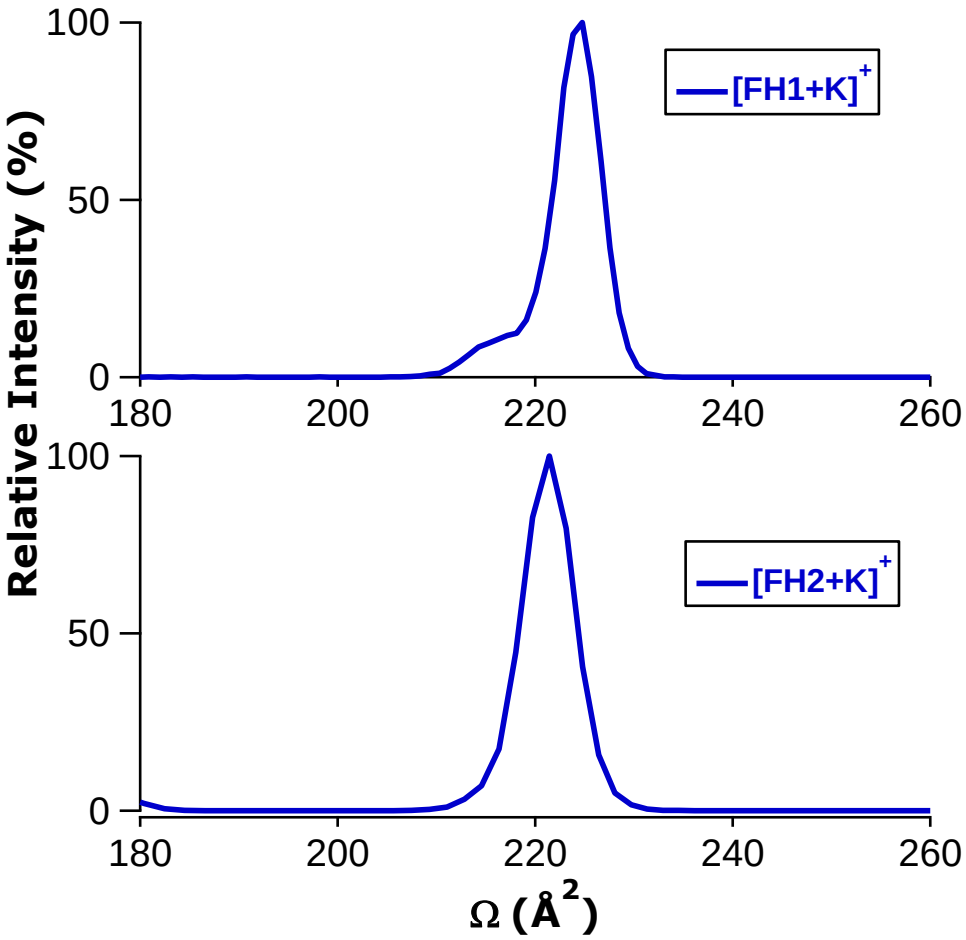

Figure S36. Representative distributions of ion-neutral CCS values for FH1 and FH2 as their potassium ion adducts.

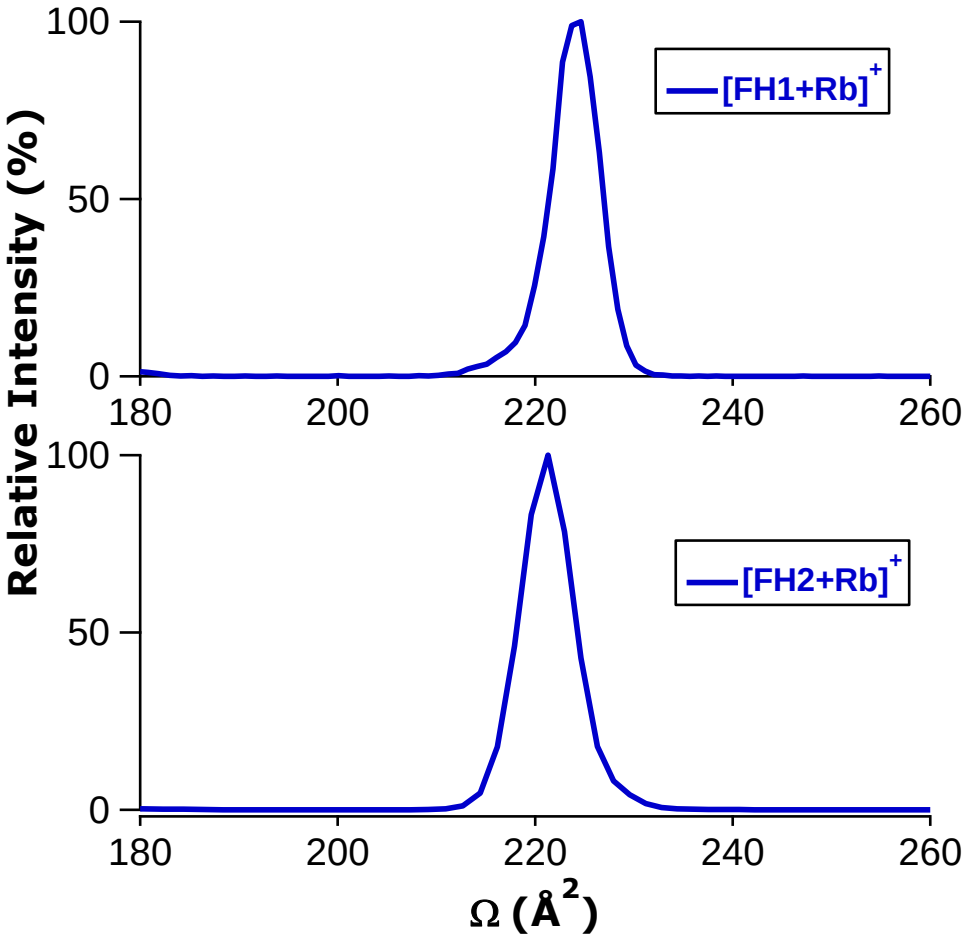

Figure S37. Representative distributions of ion-neutral CCS values for FH1 and FH2 as their rubidium ion adducts.

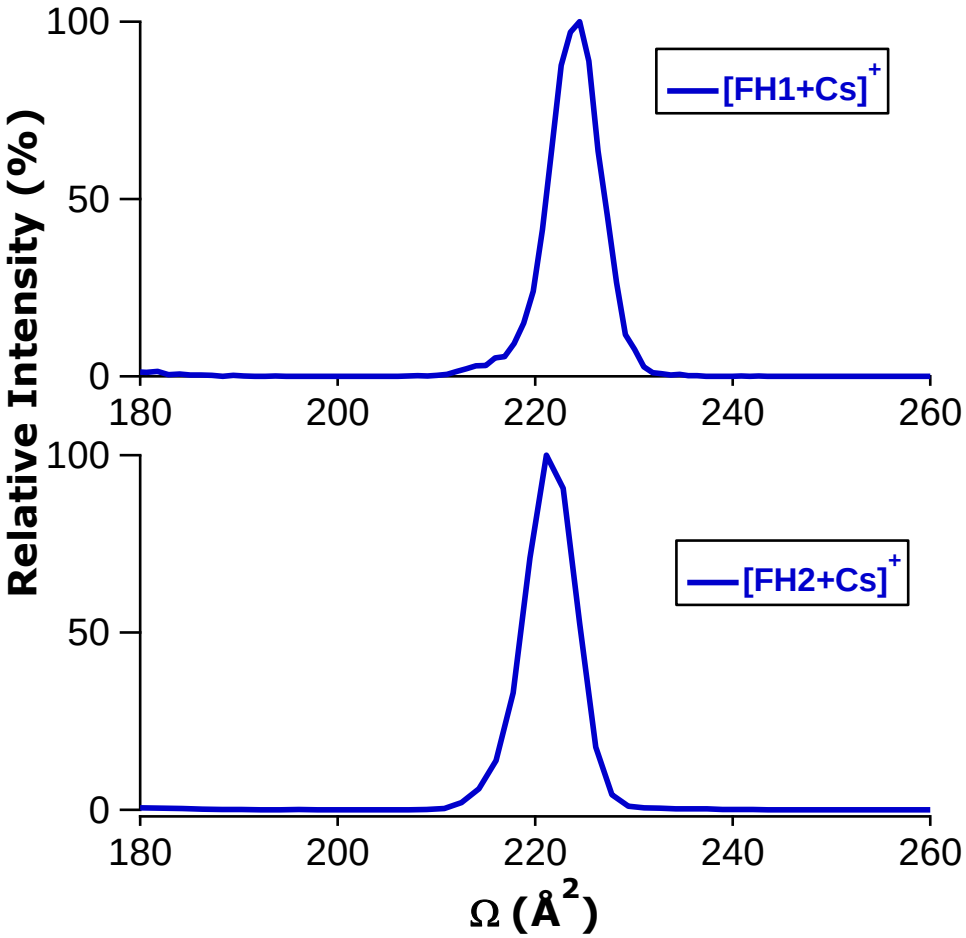

Figure S38. Representative distributions of ion-neutral CCS values for FH1 and FH2 as their cesium ion adducts.

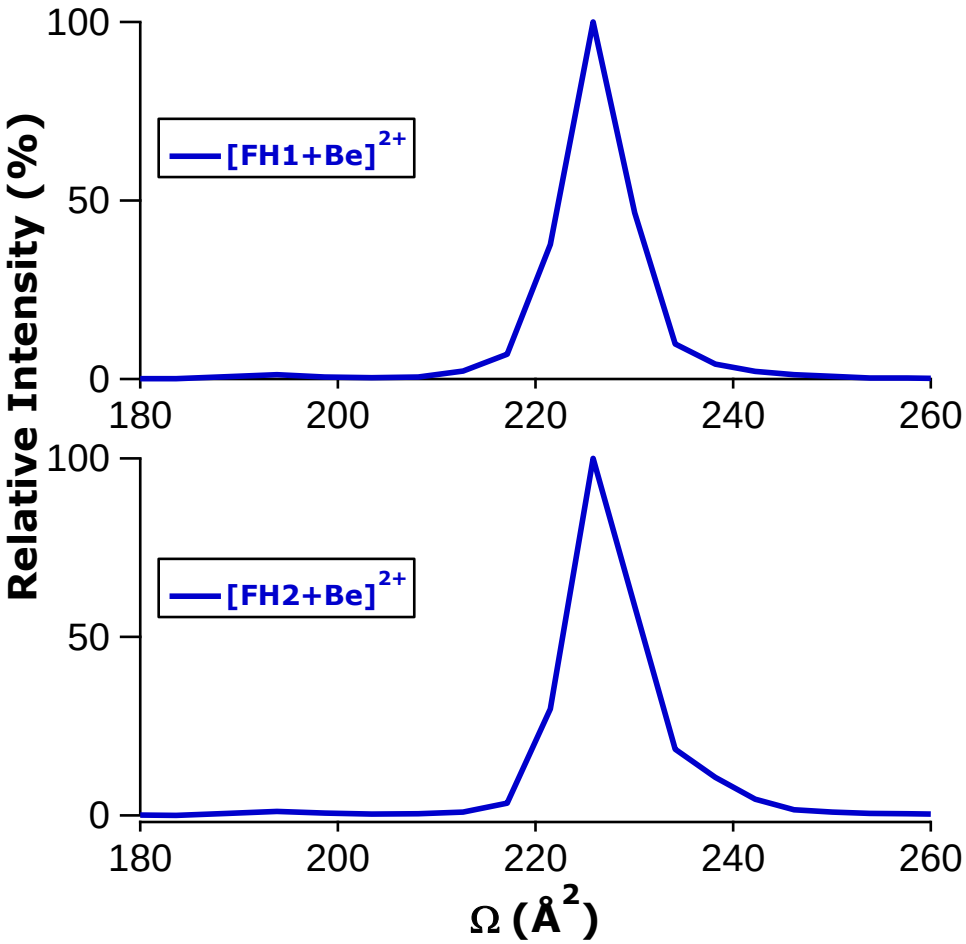

Figure S39. Representative distributions of ion-neutral CCS values for FH1 and FH2 as their beryllium ion adducts.

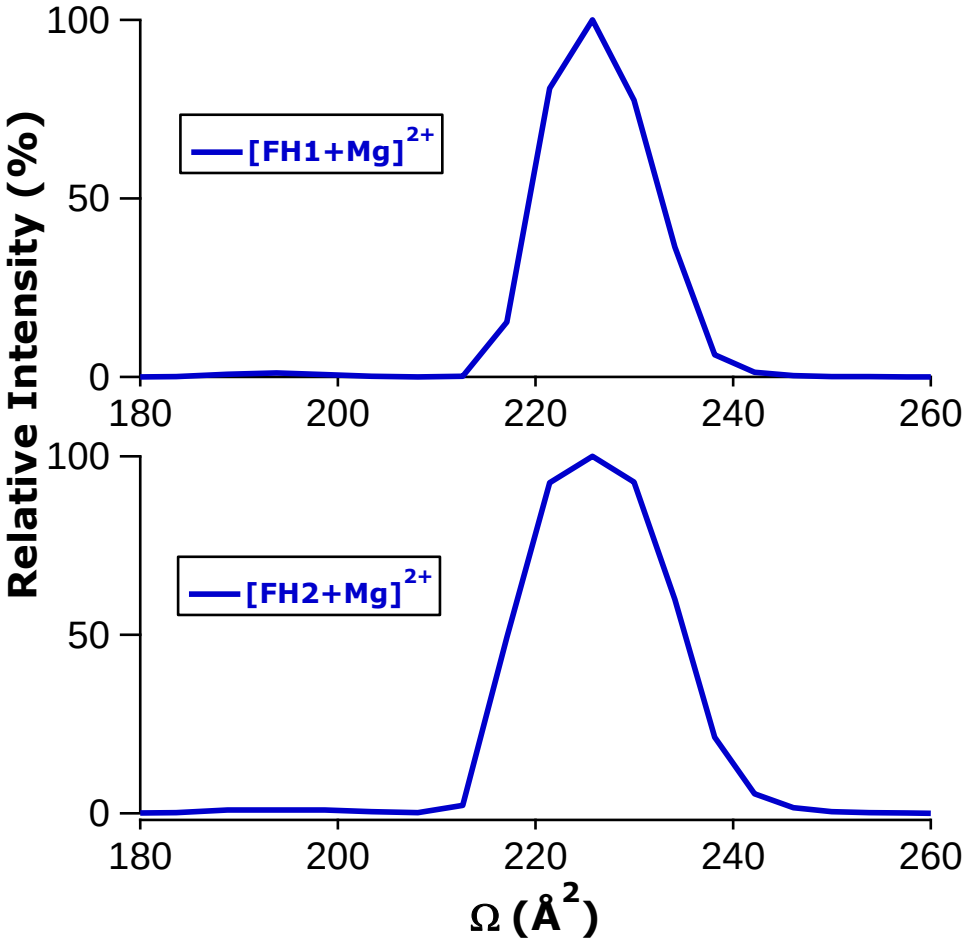

Figure S40. Representative distributions of ion-neutral CCS values for FH1 and FH2 as their magnesium ion adducts.

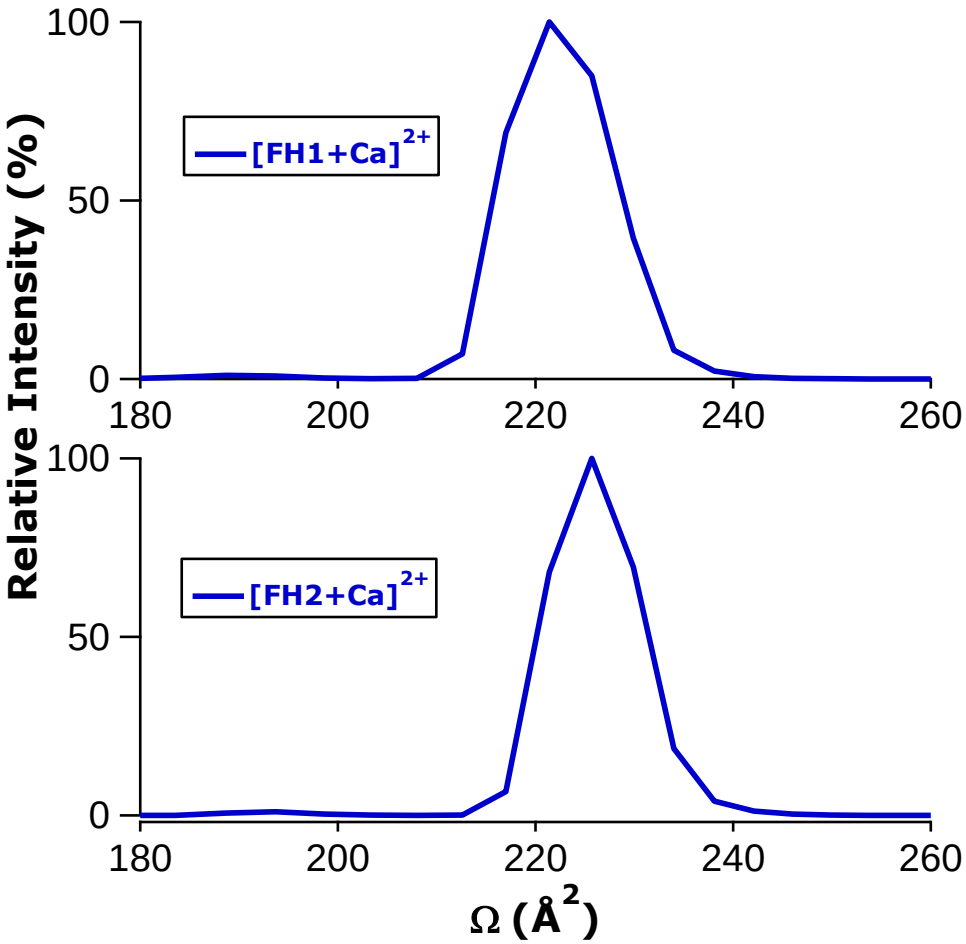

Figure S41. Representative distributions of ion-neutral CCS values for FH1 and FH2 as their calcium ion adducts.

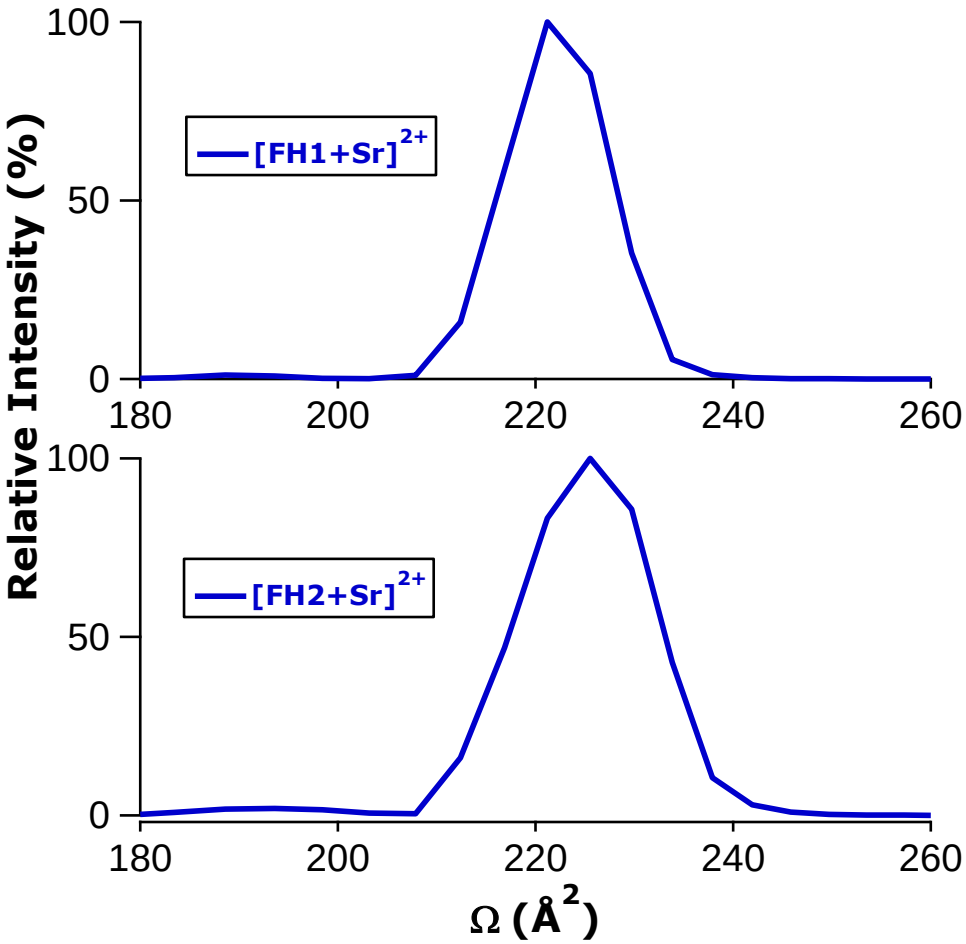

Figure S42. Representative distributions of ion-neutral CCS values for FH1 and FH2 as their strontium ion adducts.

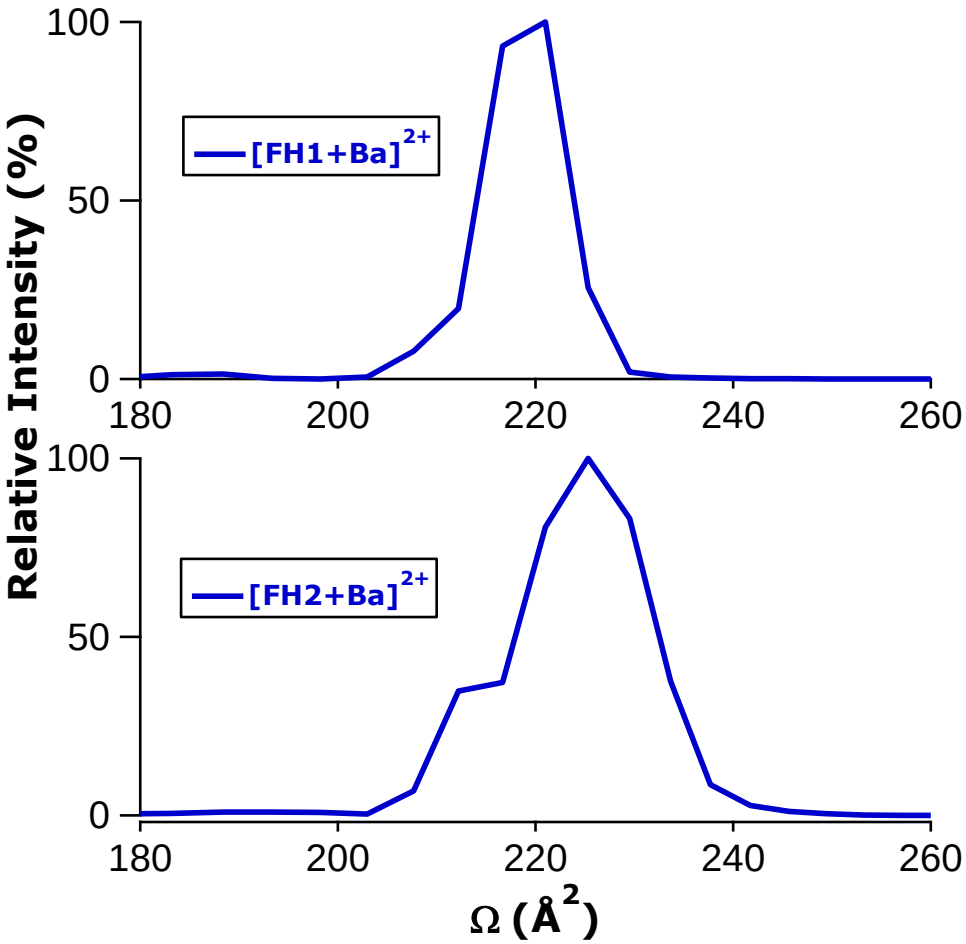

Figure S43. Representative distributions of ion-neutral CCS values for FH1 and FH2 as their barium ion adducts.

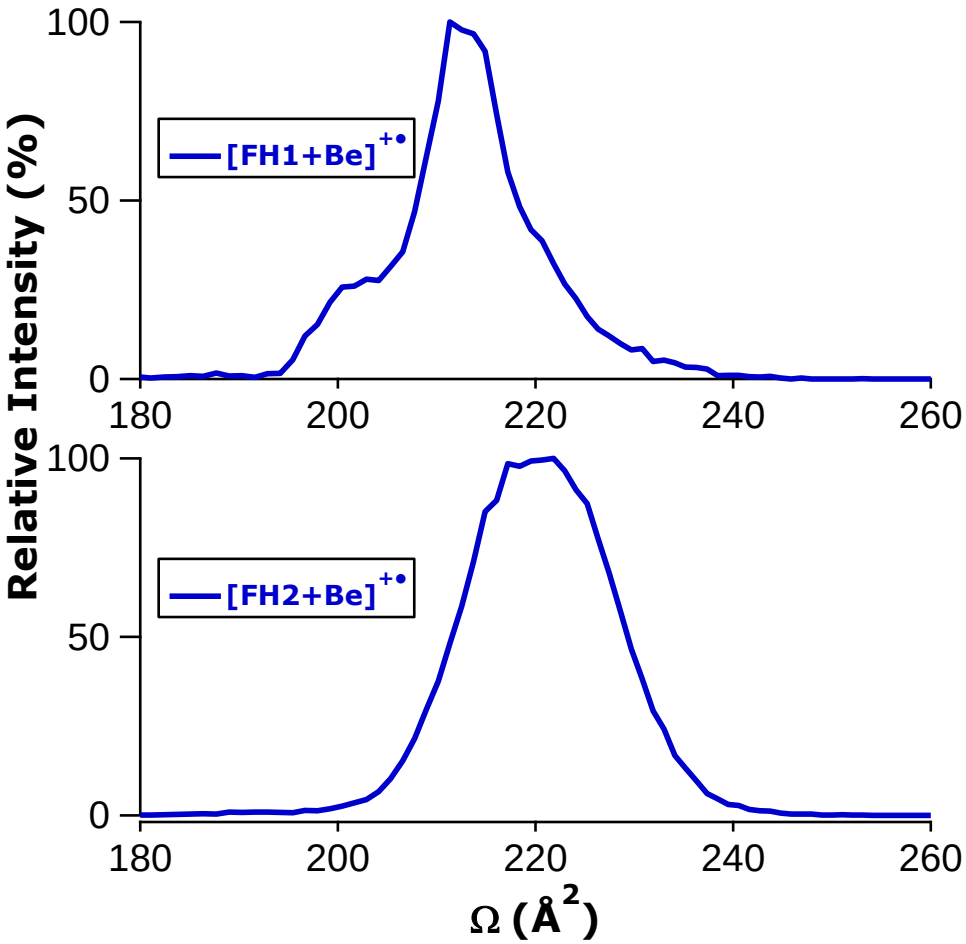

Figure S44. Representative distributions of ion-neutral CCS values for FH1 and FH2 as the ET products of their beryllium ion adducts.

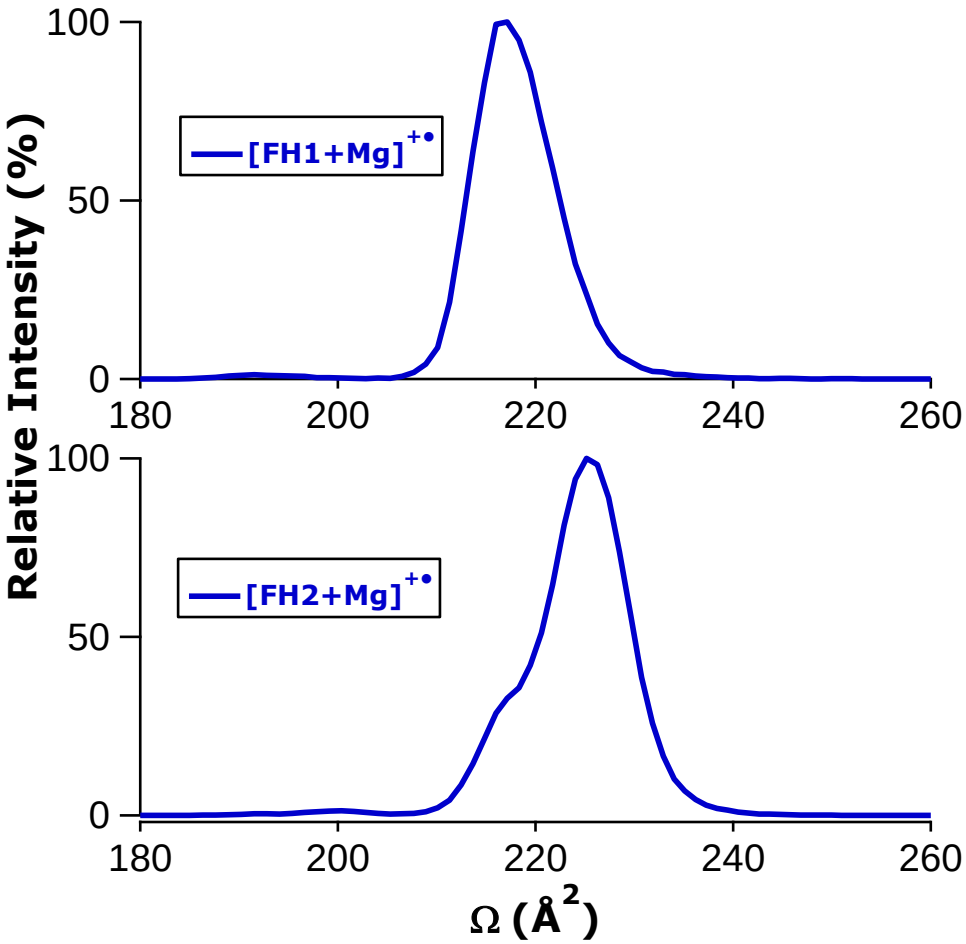

Figure S45. Representative distributions of ion-neutral CCS values for FH1 and FH2 as the ET products of their magnesium ion adducts.

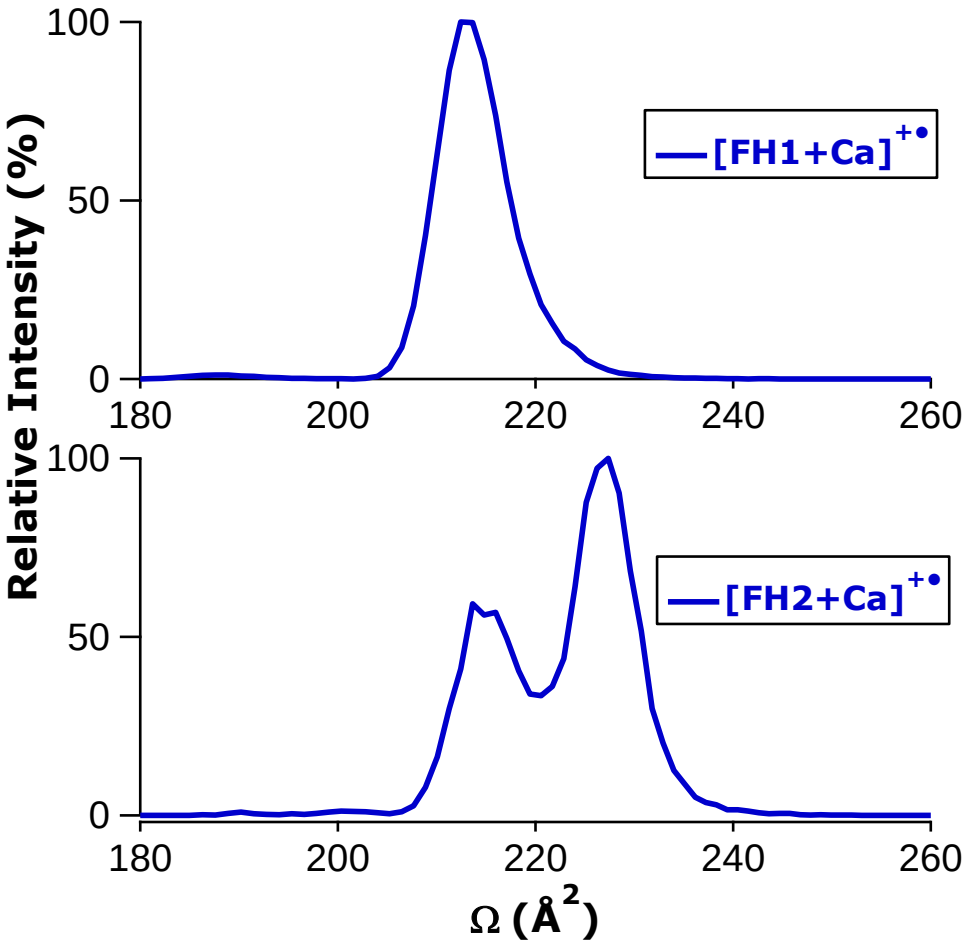

Figure S46. Representative distributions of ion-neutral CCS values for FH1 and FH2 as the ET products of their calcium ion adducts.

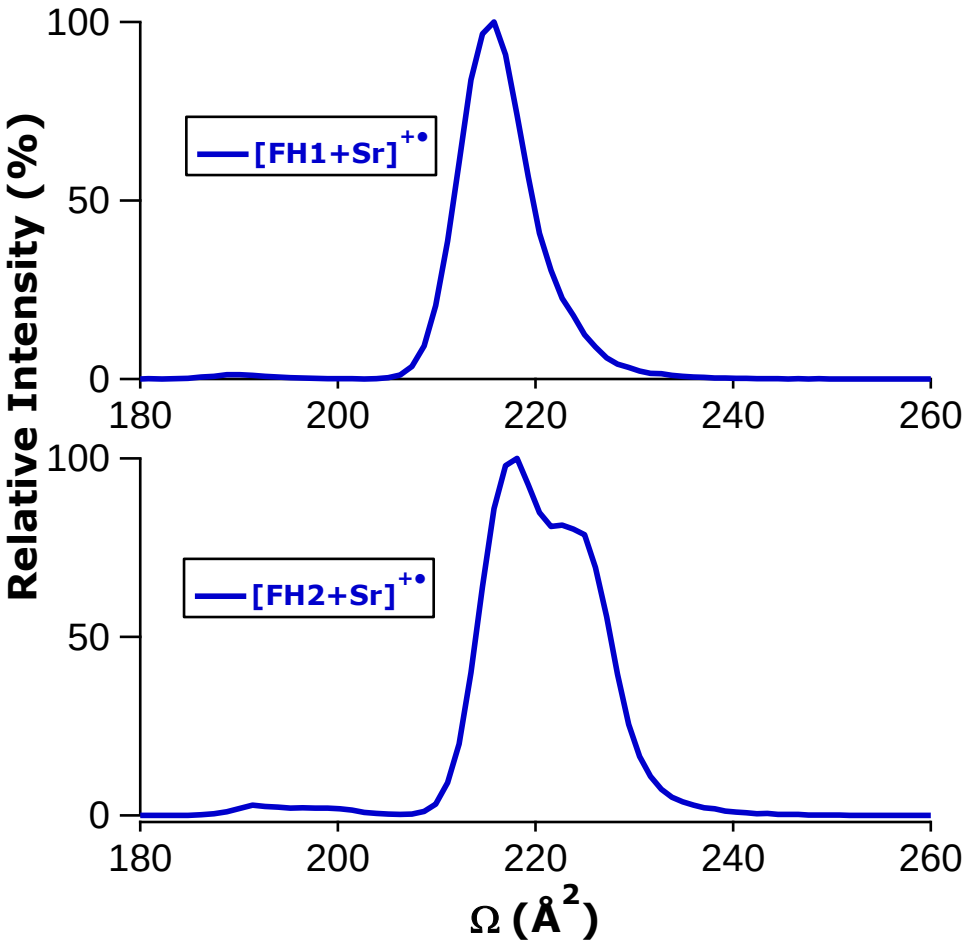

Figure S47. Representative distributions of ion-neutral CCS values for FH1 and FH2 as the ET products of their strontium ion adducts.

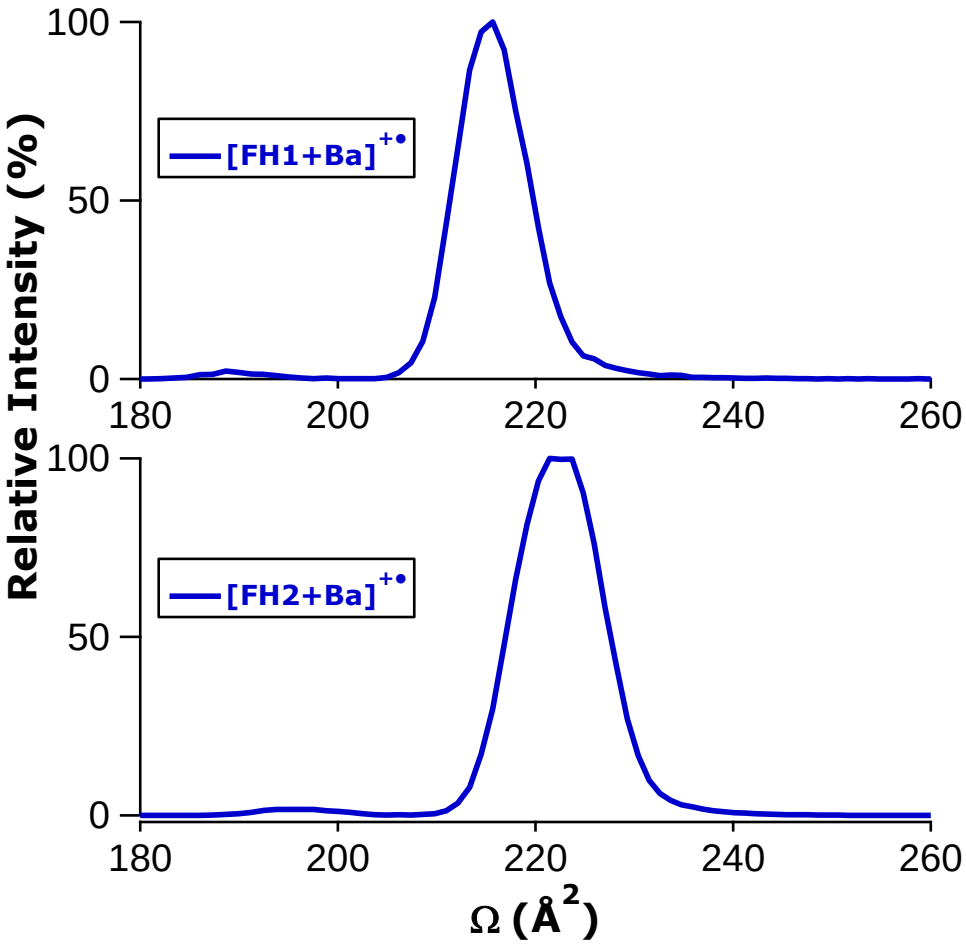

Figure S48. Representative distributions of ion-neutral CCS values for FH1 and FH2 as the ET products of their barium ion adducts.